

Competing orders in coupled Luttinger liquids

Congjun Wu,^{1,2} W. Vincent Liu,^{1,3} and Eduardo Fradkin¹

¹*Department of Physics, University of Illinois at Urbana-Champaign, Urbana, Illinois 61801-3080, USA*

²*Department of Physics, McCullough Building, Stanford University, Stanford, California 94305-4045, USA*

³*Department of Physics, Massachusetts Institute of Technology, Cambridge, Massachusetts 02139-4307, USA*

(Received 13 June 2002; revised manuscript received 7 April 2003; published 10 September 2003)

We consider the problem of two-coupled Luttinger liquids both at half filling and at low doping levels, to investigate the problem of competing orders in quasi-one-dimensional strongly correlated systems. We use bosonization and renormalization group equations to investigate the phase diagrams, to determine the allowed phases, and to establish approximate boundaries among them. Because of the chiral translation and reflection symmetries in the charge mode away from half filling, orders of charge-density wave (CDW) and spin Peierls (SP), diagonal current (DC), and d -density wave (DDW) form two doublets and thus can be at most quasi-long-range ordered. At half filling, Umklapp terms break this symmetry down to a discrete group and thus Ising-type ordered phases appear as a result of spontaneous breaking of the residual symmetries. Quantum disordered Haldane phases are also found, with finite amplitudes of pairing orders and triplet counterparts of CDW, SP, DC, and DDW. Relations with recent numerical results and implications to similar problems in two dimensions are discussed.

DOI: 10.1103/PhysRevB.68.115104

PACS number(s): 71.10.Fd, 71.10.Hf, 71.30.+h, 74.20.Mn

I. INTRODUCTION

The problem of the nature of the phase diagram of the cuprate superconductors remains at the center of research in the physics of strongly correlated electron systems. A recent work has focused on the possible competing orders responsible for the known features of the phase diagram as well as the unusual physical properties of the pseudo-gap regime. A number of candidate competing orders have been considered, including antiferromagnetism, d -wave pairing (DSC), incommensurate charge-ordered states and other liquid crystal-like phases, and d -density wave states (DDW) [also known as staggered flux states (SF) or orbital antiferromagnetism (OAF)], among others.

SO(5) theory¹ focuses on the competition between antiferromagnetism and d -wave superconductivity. In this theory, the natural SU(2)×U(1) symmetry of the spin and charge degrees of freedom is regarded as the result of an explicit symmetry breaking of a larger symmetry, characterized by a global SO(5) group. In this picture, this larger symmetry is not apparent except close to a quantum critical point whose quantum fluctuations suppress both antiferromagnetism and d -wave superconductivity, thus leading to a pseudogap regime controlled by this fixed point.

In contrast, in the stripe mechanism,² the ground state of the doped Mott insulator is an inhomogeneous charge ordered state resembling a liquid crystal phase,³ which breaks both rotational invariance and (partially) translation invariance, i.e., it is a quantum smectic. In this picture, the pseudogap is the spin gap which develops in these quasi-one-dimensional states, and it is not a signature of some sort of long-range order. In this mechanism, macroscopic phase coherence and d -wave superconductivity result from interstripe Josephson couplings.^{2,4}

In the d -density wave state, and similarly in the physically equivalent staggered flux and orbital antiferromagnetic states, there is a hidden order which has the same $d_{x^2-y^2}$

symmetry as a d -wave superconductor. In this phase, the ground state has an ordered pattern of staggered orbital currents, and this is the order which competes with d -wave superconductivity.⁵⁻¹⁰

However, in spite of a continued effort during the past decade or so, and largely due to the lack of systematic non-perturbative methods in two dimensions, it has been quite difficult to establish the phase diagram of reasonable two dimensional strongly correlated systems based on the Hubbard model. Much of the work done is based on mean-field-type approximations which favor one type of order over others or privileges the competition among a particular pair of order parameters. While it is quite possible that these studies reveal different aspects of possible phase diagrams of some generic, possibly short-range models, it is not possible at present to determine reliably the phase diagram of many of these models except sometimes at extreme regimes of some parameter. Thus, different approaches, including large- N methods (and their relatives), have been used to construct spin-liquid states.¹¹⁻¹⁷ Hartree-Fock, large- d , and large- N methods have been used to study phase separation and striped states.¹⁸⁻²¹ Similarly, Hartree-Fock methods have also been used to study the competition between superconductivity and DDW order.²² There is also an extensive literature on numerical simulations which work either at moderate to high temperatures (as in Quantum Monte Carlo simulations due to the fermion sign problem) or at exact diagonalizations of systems which are usually too small to resolve these issues.

It is largely for these reasons, as well as for the need of nonperturbative results, that some of these questions have been considered in the framework of quasi-one-dimensional systems such as Hubbard-type models (in a loose sense) on chains and ladders. Many of these issues, but not all, can be studied in quasi-one-dimensional systems. However, not all of these questions can be addressed in one dimension as the physics may be quite different. For instance, the two-

dimensional spin-liquid states in two dimensions have very specific features with no counterpart in one dimension (not even in ladders).^{23–25} Likewise, the description of a doped one-dimensional Mott insulator at weak coupling is a Luttinger liquid, while at strong coupling it is an incommensurate soliton crystal which is also a Luttinger liquid, albeit with strongly renormalized parameters. In contrast, in two dimensions, at weak coupling one may expect to find Fermi-liquid pockets, while at stronger couplings there is a host of possible liquid crystal like phases going from a solid to a stripe (or smectic) to a nematic, whose behavior is markedly different from their one-dimensional counterparts (when they exist). Nevertheless, and in spite of these caveats, studies of quasi-one-dimensional systems have yielded a wealth of information on the physics of strongly correlated systems.

The simplest quasi-one-dimensional systems for the study of some of the competing orders described above (and others) are ladder systems. Away from half filling, Hubbard-type models on ladder systems can be reduced to the problem of two-coupled Luttinger liquids. There is by now a rather extensive literature on the properties of coupled Luttinger liquids. These systems have been studied both analytically^{26–36} and numerically^{37–42} partly for their theoretical simplicity as well as a laboratory to test ideas intended to work possibly in two dimensions, and for their relevance to ladder compounds.⁴³ As it turns out, systems of two-coupled Luttinger liquids can support almost all of the local orders proposed for two-dimensional systems and thus shed some light on them. It is thus interesting to investigate this setting as the competition between different sorts of possible ordered states, to investigate their phase diagrams systematically and to compare with numerical results.

In this paper, we investigate the phase diagrams of two weakly coupled Luttinger liquids both at low doping levels and at half filling, using bosonization and renormalization group (RG) methods. A number of authors have considered before many aspects of this problem (see, in particular, Refs. 29–33,35,36). Although many of the phases that we will discuss here have been discussed before, we also find a number of different and interesting phases as well as a number of new symmetry relations between some of these phases.

One of the motivations of this paper was the recent suggestion that the Ising-like order parameter of the Z_2 symmetry of the DDW phase could be observed separately from the incommensuration associated with varying the doping level.^{7,8,22} If this was true, it may be possible to have a stable phase on a ladder with spontaneously broken Z_2 . Unfortunately, and in agreement with recent results by Fjarestad and Marston,³⁶ we find that while the DDW order parameter does contain an Ising-like piece (as it should), it always involves the charge degree of freedom which leads to incommensurate behavior. On a ladder, this leads to correlation function which decays like a power of the distance. Although our results were derived at weak coupling we expect that this behavior should extend to strong coupling, as well (with the usual large but finite renormalizations of velocities and exponents.) However, in two dimensions, this implies at least two (and possibly more) possible and distinct phases: a Fermi-liquid-like DDW phase with pockets,^{7,8} and a smectic

(or stripe) phase with DDW order. We also find that it is quite hard to reach this phase in a ladder system, at least within a naive derivation of the effective bosonized theory from Hubbard-like microscopic models, which we summarize in Appendix A. Recent, unpublished, numerical simulations by Troyer, Chakravarty, and Schollwöck⁴² have reached similar conclusions although in a regime where the couplings are larger. These authors find exponentially decaying correlations and hence only short-range DDW order, which means that the simulations reflect a quantum disordered phase (of the type described below). (See also the recent work of Stanescu and Phillips.⁴⁴)

The intertwining of charge order with some other sort of order (with a discrete symmetry group) is obviously not peculiar to DDW order. This is a rather generic situation which leads to interesting phases. It also happens for instance, and this is well known, to the Spin-Peierls or dimerized phase which, upon doping in two dimensions, also becomes either a Fermi liquid driven by Fermi-surface pockets at weak coupling or a liquid crystal phase, such as a stripe state, at intermediate and strong coupling. One such example is a bond-centered stripe state which was considered at some length by Vojta, Zhang, and Sachdev,²¹ or a site-centered stripe of the type considered by Granath and co-workers⁴ which has a rich phase diagram. In a ladder system, these phases are Luttinger liquid which cannot be qualitatively distinguished from their weak coupling counterparts.

We also find a number of interesting symmetries relating pairs of these phases. We find that, away from half filling, the charge-density wave phase (CDW) with the spin-Peierls phase (SP) (or bond-density wave) and a diagonal current phase (DC) (described below) with the commensurate DDW phase form two doublets under the continuous symmetry of sliding the charge profile, represented by the uniform chiral shift of the charge Luttinger field $\phi_{c+} : \phi_{c+} \rightarrow \phi_{c+} + \alpha \pmod{4\sqrt{\pi}}$, $\phi_{c\pm} \rightarrow -\phi_{c\pm}$ (where the real number α is an arbitrary phase), i.e., a chiral translation on a circle and a reflection. This continuous symmetry group is non-Abelian and it may be denoted by $C_{\infty v}$, in Schoenflies' symbols. Since in one-dimensional quantum systems continuous symmetries cannot be broken spontaneously, they can only exhibit at most quasi-long-range fluctuating order and power-law correlations. However, at half-filling, Umklapp terms break the continuous symmetry $C_{\infty v}$ down to the finite group C_{4v} , i.e., $\phi_{c+} \rightarrow \phi_{c+} + n\sqrt{\pi} \pmod{4\sqrt{\pi}}$ and $\phi_{c\pm} \rightarrow -\phi_{c\pm}$. Hence, at half filling, these symmetries can be broken spontaneously leading to true long-range ordered Ising-type phases. In addition, we also find four quantum disordered Haldane-like phases whose low-energy physics can be described by a suitable $O(3)$ nonlinear σ model. In these phases, there is a spin gap which remains present away from half filling. In this regime, these phases are Luther-Emery liquids. There are considerable numerical and analytic evidences for these spin-gap phases which are in agreement with our conclusions.^{37–39,43} We also discuss in detail the nature of the quantum phase transitions found at half filling.

This paper is organized as follows. In Sec. II, we present the effective Hamiltonians and the order parameters used below to characterize the different phases in their bosonized

form. In Sec. III, we use a renormalization group analysis and the known strong-coupling behaviors of the effective theory at low doping level to construct a phase diagram. In Sec. IV, we do the same type of analysis as in Sec. III but at half filling. In Sec. V, we present our conclusions. In Appendix A, we relate the parameters of the effective bosonized theory with those of the extended Hubbard model on the ladder, and in Appendix B we give explicit expressions for the order parameters of interest in terms of the bosonic fields.

II. MODEL HAMILTONIANS AND ORDER PARAMETERS

We begin with two-coupled one-dimensional chains. To a large extent, we will follow the approach used by Schulz in Ref. 29. We consider first the noninteracting limit, and diagonalize the kinetic part in terms of “bonding” and “antibonding” bands (denoted by 1 and 2, respectively), i.e., symmetric and antisymmetric under the exchange of the chain labels. Including nearest-neighbor hopping, the noninteracting dispersion relations are just $\epsilon_{i\sigma}(k) = -2t\cos k \mp t_{\perp}$ ($i=1,2$), where t_{\perp} is the interchain hopping integral. This approach makes sense if t_{\perp} is large compared to any of the dynamically generated gaps of the system, i.e., in the weakly interacting limit.

To first order in the doping level δ , the Fermi wave vectors of two bands are, respectively, $k_{f1,2a} = \pi(1-\delta)/2 \pm \sin^{-1}(t_{\perp}/2t)$, and the corresponding bare Fermi velocities are $v_{f1,2}/a = \sqrt{4t^2 - t_{\perp}^2} \pm t_{\perp} \delta\pi/2$, where a is the lattice constant which will serve as the short distance cutoff in the bosonized theory. We will consider the regimes of both low doping and half filling (discussed in Secs. III and Sec. IV, respectively) and assume that t_{\perp} is not necessarily small. At half filling where the Umklapp processes dominate, the system has the particle-hole symmetry

$$v_{f1} = v_{f2} \quad \text{and} \quad k_{f1} + k_{f2} = \pi. \quad (2.1)$$

Away from half filling, we will assume that the doping level δ is large enough to suppress the effects of all Umklapp processes (See Sec. III). However, if δ is relatively small, the relation Eq. (2.1) still holds approximately. In this regime the difference in their Fermi velocities does not play a very important role (see, however, the discussion in Ref. 45). However, as the filling factor of one of the bands approaches zero, the respective Fermi velocity becomes very small and the physics is somewhat changed. In this limit, there is an enhancement of the processes leading to the formation of a spin gap.^{2,32} Since we will also find spin-gap phases, we will ignore here this special regime since it leads to the same physics (albeit with very different parameters).

The effective theory then consists of two-coupled Luttinger liquids, for the bonding and antibonding bands, and a set of perturbations, which we describe below, each associated with a particular coupling constant. In Appendix A, we will relate these coupling constants with the interaction parameters of an extended Hubbard model on a ladder with hopping amplitudes t and t_{\perp} , on-site Hubbard repulsion U , and Coulomb interactions V_{\parallel} (on the chains), V_{\perp} (on the rungs), and V_d (along the diagonals of the elementary

plaquette), as well as the exchange Heisenberg interactions J_{\parallel} (on the chains) and J_{\perp} (on the rungs).

We bosonize the effective theory by introducing a charge bose field and a spin bose field for both the bonding and antibonding Fermi fields, $\phi_{\nu,i}$, where $i=1,2$ and $\nu=c,s$, where c and s label charge and spin modes, respectively. These fields are mixed under the effects of various interactions, in particular, the backscattering coupling of the respective charge and spin currents and densities. The bosonized theory is diagonalized in terms of the even and odd combinations of bose fields from each band: $\phi_{\nu\pm} = (\phi_{\nu,1} \pm \phi_{\nu,2})/\sqrt{2}$, $\theta_{\nu\pm} = (\theta_{\nu,1} \pm \theta_{\nu,2})/\sqrt{2}$, $\nu=c,s$.

The quadratic parts of the Hamiltonian density have the standard “universal” form:

$$\begin{aligned} \mathcal{H}_{c,\pm} &= \frac{v_{c,\pm}}{2} \left[K_{c,\pm} \Pi_{c,\pm}^2 + \frac{1}{K_{c,\pm}} (\partial_x \phi_{c,\pm})^2 \right], \\ \mathcal{H}_{s\pm} &= \frac{v_{s,\pm}}{2} \left[K_{s,\pm} \Pi_{s,\pm}^2 + \frac{1}{K_{s,\pm}} (\partial_x \phi_{s,\pm})^2 \right], \end{aligned} \quad (2.2)$$

where $\Pi_{\nu,\pm}$ are the momenta canonically conjugate to the bose fields $\phi_{\nu,\pm}$. The effective Luttinger parameters and velocities $v_{c,\pm}$ and $v_{s,\pm}$ are given by

$$\begin{aligned} K_{c\pm} &= \sqrt{\frac{2\pi v_f \mp g_{c\pm}}{2\pi v_f \pm g_{c\pm}}}, \quad K_{s\pm} = \sqrt{\frac{2\pi v_f \pm g_{s\pm}}{2\pi v_f \mp g_{s\pm}}}, \\ v_{c,\pm} &= \sqrt{v_f^2 - \left(\frac{g_{c\pm}}{2\pi}\right)^2}, \quad v_{s,\pm} = \sqrt{v_f^2 - \left(\frac{g_{s\pm}}{2\pi}\right)^2}, \end{aligned} \quad (2.3)$$

where $v_f = (v_{f1} + v_{f2})/2$. The coupling constants $g_{c\pm}$, $g_{s\pm}$ correspond to forward-scattering nonchiral couplings of the charge and spin currents, and are already taken into account in the quadratic terms. Here we have ignored the effects of straightforward effects of forward-scattering chiral couplings, since they only renormalize Fermi velocities and modify the naively determined values of the Luttinger parameters. Also note that these expressions can be taken seriously only at weak coupling. At intermediate and strong couplings, there is also a finite but significant renormalization of both the Luttinger parameters and the velocities.

Let us now discuss the nonquadratic, interaction terms. Throughout we will use Majorana Klein factors obeying the convention $\eta_{\uparrow}(1)\eta_{\downarrow}(1)\eta_{\uparrow}(2)\eta_{\downarrow}(2) = 1$. The backscattering and pair tunneling terms yield the bosonized expressions

$$\begin{aligned} \mathcal{H}_{int} &= \frac{\cos\sqrt{4\pi}\phi_{s+}}{2(\pi a)^2} (g_1 \cos\sqrt{4\pi}\phi_{s-} - g_2 \cos\sqrt{4\pi}\theta_{s-}) \\ &+ \frac{\cos\sqrt{4\pi}\theta_{c-}}{2(\pi a)^2} (g_3 \cos\sqrt{4\pi}\theta_{s-} + g_4 \cos\sqrt{4\pi}\phi_{s-}) \\ &+ g_5 \cos\sqrt{4\pi}\phi_{s+}, \end{aligned} \quad (2.4)$$

where $\theta_{c,\pm}$ and $\theta_{s,\pm}$ are the dual fields of the charge bosons $\phi_{c,\pm}$ and spin bosons $\phi_{s,\pm}$, respectively. Terms labeled by

the effective coupling constants g_1 and g_2 originate from the intraband and inter-band backscattering interactions $-g_1(J_{1R}^{x,y}J_{1L}^{x,y}+1\rightarrow 2)$ and $-g_2(J_{1R}^{x,y}J_{2L}^{x,y}+1\leftrightarrow 2)$, respectively. The terms labeled by the couplings g_3 , g_4 , and g_5 represent singlet and triplet pair-tunneling processes $\lambda_s(\Delta_1^\dagger\Delta_2+\text{H.c.})$ and $\lambda_t(\vec{\Delta}_1^\dagger\vec{\Delta}_2+\text{H.c.})$ with $g_3=2\lambda_t$, $g_4=\lambda_s+\lambda_t$, and $g_5=\lambda_s-\lambda_t$. Three conditions, required by the SU(2) spin rotation invariance, relate the spin current and triplet tunneling couplings: $g_{s\pm}=(g_1\pm g_2)/2$ [see also Eq. (2.3)] and $g_5=g_4-g_3$.

Near half filling, the following additional Umklapp terms appear as

$$\begin{aligned} \mathcal{H}_{um} = & \frac{\cos(\sqrt{4\pi}\phi_{c+}-2\delta\pi x)}{2(\pi a)^2} (g_{uc}\cos\sqrt{4\pi}\theta_{c-} \\ & -g_{u3}\cos\sqrt{4\pi}\theta_{s-}-g_{u4}\cos\sqrt{4\pi}\phi_{s-} \\ & -g_{u5}\cos\sqrt{4\pi}\phi_{s+}). \end{aligned} \quad (2.5)$$

The term with coupling constant g_{uc} is the so-called ‘‘ η pair’’ tunneling processes, i.e., tunneling of Cooper pairs with momentum $2k_f$, which has the form $m_{R1}^\dagger m_{L2}+(1\rightarrow 2)+\text{H.c.}$, where $m_{R,L}=\psi_{R,L\uparrow}\psi_{R,L\downarrow}$. The terms with coupling constants g_{u3} , g_{u4} , and g_{u5} represent the couplings between the respective CDW and spin density wave (SDW) couplings on each chain: $\lambda_{cdw}(N^\dagger(1)N^\dagger(2)+\text{H.c.})$, $\lambda_{sdw}(\vec{N}^\dagger(1)\vec{N}^\dagger(2)+\text{H.c.})$, where $N(i)$ is the $2k_F$ CDW order parameter of chain $i=1,2$, and $\vec{N}(i)$ is the $2k_F$ (Néel) SDW order parameter of chain $i=1,2$. The coupling constants, which are $g_{u3}=-\lambda_{sdw}$, $g_{u4,5}=(2\lambda_{cdw}\mp\lambda_{sdw}/2)$. Due to the SU(2) spin symmetry, condition $g_{u5}=g_{u4}-g_{u3}$ also holds.

For the two-leg ladder, we only consider where repulsive interactions dominate, which implies that the bare values of the effective Luttinger parameters are in the regime $K_{c+}(0)\ll 1$, $K_{c-}(0), K_{s-}(0)\sim 1$. Compared with Ref. 29, $K_{c-}(0), K_{s-}(0)$ are not necessarily 1, for here they are determined by off-site interactions (see Appendix A).

Bosonic expressions for various order parameters are given in Appendix B. In the particle-hole (p - h) channel, the possible singlet fermionic bilinear forms, which break the translational symmetry, are the order parameters for the CDW and SP, DC, and DDW operators as shown in Fig. 1. The CDW and SP order parameters are proportional to the real and imaginary parts of the symmetric bilinear $\psi_{1L\sigma}^\dagger\psi_{2R\sigma}+\psi_{2L\sigma}^\dagger\psi_{1R\sigma}$, whereas the DC and DDW order parameters are the real and imaginary parts of the antisymmetric version of this bilinear.

From their bosonic representations, we find that all four order parameters transform nontrivially under the symmetries broken in their associated phases (or ground states). Thus, for instance, the SP and DDW order parameters are odd under the \mathbb{Z}_2 symmetries broken spontaneously by the SP and DDW phases. However, in all four cases, these order parameters also involve a phase factor (or vertex operator) of the charge boson $\phi_{c,+}$. Hence, these order parameters also transform nontrivially under shifts of the charge boson $\phi_{c,+}$,

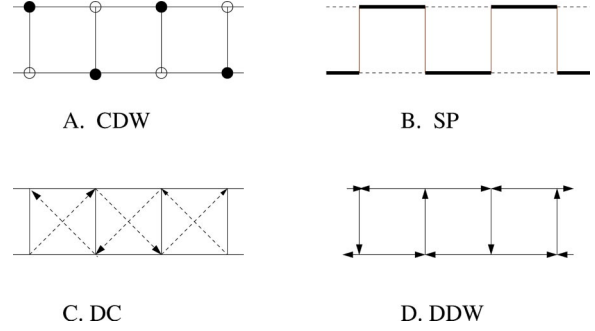


FIG. 1. Four Ising type phases. A. charge-density wave (CDW), B. spin-Peierls (SP); C. diagonal current (DC), D. d-density wave (DDW). Their triplet analogs are denoted as SDW, SP^t; DC^t, DDW^t respectively.

i.e., uniform displacements of the charge profile. This dependence means that the discrete symmetries, broken spontaneously in these phases with long-range order, are intertwined with the continuous symmetry of the incommensurate doped state. Consequently, these order parameters do not truly acquire an expectation value but instead only display power-law correlations. Also, while it is possible to write down bosonic expressions for operators which transform only under the discrete symmetries broken by these phases, their fermionic versions are strongly nonlocal. Hence, we conclude that these orders are always incommensurate.

We also find that these order parameters also form two doublets of the $C_{\infty v}$ group. Similarly, their triplet counterparts SDW, SP^t, DC^t, and DDW^t are proportional to real and imaginary parts of $\psi_{1L\alpha}^\dagger(\vec{\sigma}/2)_{\alpha\beta}\psi_{2R\beta}\pm\psi_{2L\alpha}^\dagger(\vec{\sigma}/2)_{\alpha\beta}\psi_{1R\beta}$, respectively (where the label t means triplet). In the particle-particle (p - p) channel, the s - and d -wave pairing order parameters are $\Delta_{s,d}=\sum_{\sigma}(-)^{\sigma}(\psi_{1L\sigma}\psi_{1R\sigma}\pm\psi_{2L\sigma}\psi_{2R\sigma})$. In the following section, we identify the stable fixed points of the renormalization group (RG) flows for these phases associated with these order parameters.

Some of the order parameters discussed above have been investigated before in Ref. 29,30, although under different names. For example, our CDW, DDW, SDW, SSC, and DSC order parameters are called CDW ^{π} , OAF, SDW ^{π} , SC ^{s} , and SC ^{d} there. We note that in a recent paper Ref. 46, the phases that we label as DDW, SP, and DC are called SF, P -density wave and, F -density wave, respectively.

Finally, in Eq. (2.1), we ignored the effects of the following terms:

$$\Delta\mathcal{H}_c = \left(\Delta v_f + \frac{\Delta g_c}{\pi}\right)\partial_x\phi_{c+} + \partial_x\phi_{c-} + \left(\Delta v_f - \frac{\Delta g_c}{\pi}\right)\Pi_{c+}\Pi_{c-}, \quad (2.6)$$

$$\begin{aligned} \Delta\mathcal{H}_s = & \left(\Delta v_f - \frac{\Delta g_s}{\pi}\right)\partial_x\phi_{s+} + \partial_x\phi_{s-} + \left(\Delta v_f + \frac{\Delta g_s}{\pi}\right)\Pi_{s+}\Pi_{s-}, \\ & - \frac{\Delta g_s}{2(\pi a)^2}\sin\sqrt{4\pi}\phi_{s-}\sin\sqrt{4\pi}\phi_{s+}, \end{aligned} \quad (2.7)$$

TABLE I. Stable fixed points and corresponding quasi-long-range orders away from half filling, with $\langle \theta_{c-} \rangle = 0$ and $g_5 = g_4 - g_3$ [required by SU(2) invariance].

| | g_1, g_2 | g_3, g_4, g_5 | ϕ_{s+} | ϕ_{s-} | θ_{s-} | Order | Dimension |
|---|--------------|-----------------------|----------------|----------------|----------------|--------|---------------|
| 1 | 0, $-\infty$ | $+\infty, 0, -\infty$ | 0 | / | $\sqrt{\pi}/2$ | CDW+SP | $K_{c+}/4$ |
| 2 | 0, $-\infty$ | $-\infty, 0, +\infty$ | $\sqrt{\pi}/2$ | / | 0 | DC+DDW | $K_{c+}/4$ |
| 3 | $-\infty, 0$ | 0, $+\infty, +\infty$ | $\sqrt{\pi}/2$ | $\sqrt{\pi}/2$ | / | DSC | $1/(4K_{c+})$ |
| 4 | $-\infty, 0$ | 0, $-\infty, -\infty$ | 0 | 0 | / | SSC | $1/(4K_{c+})$ |

$$\Delta \mathcal{H}_{um} = \frac{\sin(\sqrt{4\pi}\phi_{c+} - 2\delta\pi x)}{2(\pi a)^2} (\Delta g_{uc} \cos\sqrt{4\pi}\theta_{c-} - \Delta g_{u3} \cos\sqrt{4\pi}\theta_{s-} - \Delta g_{u4} \cos\sqrt{4\pi}\phi_{s-} - \Delta g_{u5} \cos\sqrt{4\pi}\phi_{s+}), \quad (2.8)$$

where $\Delta v_f = \delta\pi t_\perp/2$ and all other residue coupling constants vary linearly with doping near half filling as given in Appendix A. The quadratic residual terms in Eqs. (2.6) and (2.7) are marginal perturbations, and they slightly change the scaling dimensions of various operators in Eqs. (2.4) and (2.5). Because they are small, we do not expect that they can change the stable RG fixed points associated with various phases qualitatively. For the term of Δg_s in Eq. (2.7), θ_{s+} is fixed around 0 or $\sqrt{\pi}/2$ at all the stable fixed points (see Tables I and III below). The residual Umklapp terms in Eq. (2.8) are irrelevant away from half filling. At half filling, θ_{c+} is fixed at $\sqrt{\pi}/2$ (see Table III). Thus, we conclude that all the nonquadratic operators are irrelevant at all the stable fixed points. Balents and Fisher³² used a perturbative RG of the fermionic theory and found that a spin-gap phase develops near half filling, which is consistent with the argument given above. On the other hand, the continuous $C_{v\infty}$ symmetry is preserved away from half filling where the Umklapp terms are irrelevant. Thus the conclusion that the CDW and SP, DDW, and DC order parameters are incommensurate and thus exhibit that quasi-long-range order is not affected by these terms. However, these residual terms do affect the boundaries among phases.

III. PHASE DIAGRAM IN THE INCOMMENSURATE REGIME

We will now investigate the phase diagram in the incommensurate regime, but only at low doping. In this regime, the Umklapp processes are cut off at a high-energy scale of $2\pi v_f \delta/a$, and can only yield renormalization of the param-

TABLE II. Critical phase boundaries and unstable fixed points away from half filling, also with $\langle \theta_{c-} \rangle = 0$ and $g_5 = g_4 - g_3$.

| | g_{s+}, g_{s-} | g_3, g_4, g_5 | ϕ_{s+} | Transition |
|---|------------------|-----------------------------|----------------|------------------------------|
| 1 | 0, 0 | $+\infty, +\infty, 0$ | unfixed | CDW+SP \leftrightarrow DSC |
| 2 | 0, 0 | $-\infty, -\infty, 0$ | unfixed | DDW+DC \leftrightarrow SSC |
| 3 | $-\infty, 0$ | $-\infty, +\infty, +\infty$ | $\sqrt{\pi}/2$ | DDW+DC \leftrightarrow DSC |
| 4 | $-\infty, 0$ | $+\infty, -\infty, -\infty$ | 0 | CDW+SP \leftrightarrow DSC |

eters such as the velocities, coupling constants, and Luttinger parameters of the low-energy effective theory. The contributions from the Umklapp terms in the RG equations away from half filling⁴⁷ are given in terms of Bessel functions, which oscillate when an energy scale lower than that of the Umklapp process is reached. At this scale, the effects of these terms can be neglected. Below, we begin directly at the low-energy scale with all the coupling constants and Luttinger parameters already renormalized by the Umklapp terms.

We will investigate the role of the remaining interactions by means of a one-loop renormalization group (RG) analysis combined with semiclassical arguments. In this regime, the charge boson ϕ_{c+} essentially decouples and remains gapless. Thus, to one-loop order, the Luttinger parameter K_{c+} does not flow. (This argument is not completely correct: there are always irrelevant couplings which do lead to finite renormalizations of K_{c+} ; these effects do not show up at one-loop order.)

TABLE III. Fixed points at half filling: Stable fixed points and corresponding gapped phases. We have set $\langle \phi_{c+} \rangle = \sqrt{\pi}/2$. The SU(2) condition requires $g_5^* = g_4^* - g_3^*$. Phases 1,2,5,6 have true Ising-type long-range order, while 3,4,7,8 are quantum disordered Haldane-like phases.

| | g_{uc} | g_1, g_2 | g_3^*, g_4^*, g_5^* | θ_{c-} | ϕ_{s+} | (ϕ_{s-}, θ_{s-}) | phase |
|---|-----------|--------------|-----------------------|------------------------|------------------------|-----------------------------|----------------------|
| 1 | $+\infty$ | 0, $-\infty$ | $+\infty, 0, -\infty$ | 0 | 0 | $(/, \frac{\sqrt{\pi}}{2})$ | SP |
| 2 | $+\infty$ | 0, $-\infty$ | $-\infty, 0, +\infty$ | 0 | $\frac{\sqrt{\pi}}{2}$ | $(/, 0)$ | DDW |
| 3 | $+\infty$ | $-\infty, 0$ | 0, $+\infty, +\infty$ | 0 | $\frac{\sqrt{\pi}}{2}$ | $(\frac{\sqrt{\pi}}{2}, /)$ | DSC+SDW |
| 4 | $+\infty$ | $-\infty, 0$ | 0, $-\infty, -\infty$ | 0 | 0 | $(0, /)$ | SSC+DC ^t |
| 5 | $-\infty$ | 0, $-\infty$ | $-\infty, 0, +\infty$ | $\frac{\sqrt{\pi}}{2}$ | $\frac{\sqrt{\pi}}{2}$ | $(/, 0)$ | CDW |
| 6 | $-\infty$ | 0, $-\infty$ | $+\infty, 0, -\infty$ | $\frac{\sqrt{\pi}}{2}$ | 0 | $(/, \frac{\sqrt{\pi}}{2})$ | DC |
| 7 | $-\infty$ | $-\infty, 0$ | 0, $-\infty, -\infty$ | $\frac{\sqrt{\pi}}{2}$ | 0 | $(0, /)$ | DSC+SP ^t |
| 8 | $-\infty$ | $-\infty, 0$ | 0, $+\infty, +\infty$ | $\frac{\sqrt{\pi}}{2}$ | $\frac{\sqrt{\pi}}{2}$ | $(\frac{\sqrt{\pi}}{2}, /)$ | SSC+DDW ^t |

The one-loop RG equations for the coupling constants g_1 through g_5 and Luttinger parameters $K_{c,-}$ and $K_{s,\pm}$ are

$$\begin{aligned}
 \frac{dK_{c-}}{dl} &= \frac{1}{8\pi^2}(g_3^2 + g_4^2 + g_5^2), \\
 \frac{dK_{s+}}{dl} &= -\frac{K_{s+}^2}{8\pi^2}(g_1^2 + g_2^2 + g_5^2), \\
 \frac{dK_{s-}}{dl} &= -\frac{K_{s-}^2}{8\pi^2}(g_1^2 + g_4^2) + \frac{1}{8\pi^2}(g_2^2 + g_3^2), \\
 \frac{dg_1}{dl} &= (2 - K_{s+} - K_{s-})g_1 - \frac{g_4 g_5}{2\pi}, \\
 \frac{dg_2}{dl} &= \left(2 - K_{s+} - \frac{1}{K_{s-}}\right)g_2 + \frac{g_3 g_5}{2\pi}, \\
 \frac{dg_3}{dl} &= \left(2 - \frac{1}{K_{c-}} - \frac{1}{K_{s-}}\right)g_3 + \frac{g_2 g_5}{2\pi}, \\
 \frac{dg_4}{dl} &= \left(2 - \frac{1}{K_{c-}} - K_{s-}\right)g_4 - \frac{g_1 g_5}{2\pi}, \\
 \frac{dg_5}{dl} &= \left(2 - \frac{1}{K_{c-}} - K_{s+}\right)g_5 - \frac{g_1 g_4}{2\pi} + \frac{g_2 g_3}{2\pi}, \quad (3.1)
 \end{aligned}$$

where $l = \ln(L/a)$ with the length scale L .

Along the SU(2)-invariant manifold for the spin current and pair tunneling terms, the RG equations can be simplified to

$$\begin{aligned}
 \frac{dK_{c-}}{dl} &= \frac{1}{8\pi^2}[g_3^2 + g_4^2 + (g_3 - g_4)^2], \\
 \frac{dg_{s+}}{dl} &= -\frac{1}{2\pi}(g_{s+}^2 + g_{s-}^2) - \frac{(g_3 - g_4)^2}{4\pi}, \\
 \frac{dg_{s-}}{dl} &= -\frac{1}{\pi}g_{s+}g_{s-} + \frac{g_3^2}{4\pi} - \frac{g_4^2}{4\pi}, \\
 \frac{dg_3}{dl} &= \left(1 - \frac{1}{K_{c-}} + \frac{-g_{s+} + 2g_{s-}}{2\pi}\right)g_3 + \frac{(g_{s+} - g_{s-})g_4}{2\pi}, \\
 \frac{dg_4}{dl} &= \left(1 - \frac{1}{K_{c-}} + \frac{-g_{s+} - 2g_{s-}}{2\pi}\right)g_4 + \frac{(g_{s+} + g_{s-})g_3}{2\pi}, \quad (3.2)
 \end{aligned}$$

with

$$\frac{d}{dl}(g_3 - g_4 + g_5) = \left(1 - \frac{1}{K_{c-}} + \frac{g_{s+}}{2\pi}\right)(g_3 - g_4 + g_5) \equiv 0. \quad (3.3)$$

These equations are invariant under transformations $(g_1, g_2, g_3, g_4) \rightarrow (g_1, g_2, -g_3, -g_4) \rightarrow (g_2, g_1, g_4, g_3)$. This means that phase boundaries must also have such symmetries.

For ‘‘bare values’’ of the Luttinger parameter $K_{c-}(0) \sim 1$, the marginally relevant RG flow of Eq. (3.2) is such that a gap develops in the $c-$ sector, which scales like $m_{c-} \approx \exp[-1/g(0)]$, where g is the most relevant one among the marginally relevant perturbations g_3 , g_4 , and g_5 . In this regime, K_{c-} flows to large values and, thus from now on we will set $1/K_{c-} = 0$. In this phase the operator $\cos(\sqrt{4\pi}\theta_{c-})$ acquires a nonvanishing expectation value, which classically is just ± 1 . Hence, in this phase the dual field takes the values $\theta_{c-} = 0, \sqrt{\pi}/2$, which are related to each other by a \mathbb{Z}_2 symmetry.³⁶ In what follows in this section, we will choose the value $\langle \theta_{c-} \rangle = 0$.

From now on, we will use the set (g_1, g_2, g_3, g_4) to represent the stable fixed points of Eq. (3.2), which are summarized in Table I. At the fixed points $(0, -\infty, \mp\infty, 0)$, the interband backscattering coupling constant g_2 is relevant, while the intraband backscattering coupling constant g_1 is irrelevant. Both λ_s and λ_t are relevant and satisfy the relation $\lambda_s = -\lambda_t$. By direct inspection of their scaling dimensions, we find that λ_s and λ_t are more relevant than g_2 . The resulting phase depends on where the RG flows go. When $g_3 \rightarrow -\infty$, the expectation values of $\phi_{s,+}$ and $\theta_{s,-}$ asymptotically take the values $\langle \phi_{s,+} \rangle = \sqrt{\pi}/2$ and $\langle \theta_{s,-} \rangle = 0$, respectively. This is the stable fixed point for either the DDW phase or the DC phase. However, this is true only for quasi-long-range order (QLRO) due to the strong fluctuations of the gapless charge boson $\phi_{c,+}$. In this phase, these order parameters have scaling dimension $K_{c,+}/4$. Conversely, when $g_3 \rightarrow +\infty$, $\langle \phi_{s,+} \rangle = 0$, and $\langle \theta_{s,-} \rangle = \sqrt{\pi}/2$. Hence, at this fixed point, we would have (naively) either a CDW phase or a spin-Peierls (or dimerized) phase. Here too this is true only for QLRO, and the associated order parameters also have scaling dimension $K_{c,+}/4$.

We conclude, in agreement with the recent results of Ref. 36, that because of the chiral translation symmetry in the field $\phi_{c,+}$, in other terms due to the charge incommensurability, there is no true long-range order of the DDW order but only (incommensurate) power-law correlations. We can further see that the DDW and DC phases (and also the CDW and SP phases) form doublet representation under the $C_{\infty v}$ group and are thus degenerate. Equivalently, the DDW and DC order parameters can be regarded as the real and imaginary parts of a single complex order parameter which can thus be rotated continuously into each other. The same relationship holds for the CDW and spin-Peierls order parameters. Thus, both stable phases CDW+SP and DDW+DC have a continuous U(1) symmetry. Naturally, since the ladder is a one-dimensional system, this symmetry is not truly spontaneously broken as there are only power-law correlations for these order parameters. However, we will see in Sec. IV that at half filling, the Umklapp terms break this symmetry explicitly from U(1) down to \mathbb{Z}_2 leading to additional Ising-like phase transitions.

Similarly, we also find that λ_s is more relevant than g_1 at $(-\infty, 0, \pm\infty)$, while g_2 and λ_t are irrelevant. When $g_4 \rightarrow +\infty$, $\langle\phi_{s+}\rangle$ and $\langle\phi_{s-}\rangle$ are fixed at $\sqrt{\pi}/2$. DSC is the leading QLRO and its order parameter has scaling dimension $1/(4K_{c+})$. Conversely, when $g_4 \rightarrow -\infty$, $\langle\phi_{s+}\rangle$ and $\langle\phi_{s-}\rangle$ are fixed at 0, s -wave superconductivity (SSC) is the leading QLRO and its order parameter also has scaling dimension $1/(4K_{c+})$.

Let us consider now the phase boundaries and the nature of the phase transitions between these possible states, at $g_{s-}(0)=0$. In this regime, it is more natural to represent instead the unstable fixed points with $(g_{s+}, g_{s-}, g_3, g_4)$. The RG flows starting with $g_{s+}(0)>0$, $g_{s-}(0)=0$, and $g_3(0)=g_4(0)=g>0$ evolve towards the fixed point at $(0, 0, +\infty, +\infty)$. Here, the field ϕ_{s+} becomes free, $K_{s\pm} \rightarrow 1$, and the residual interactions reduce to

$$\mathcal{H}_{res}^1 = \frac{g^*}{2(\pi a)^2} \langle \cos\sqrt{4\pi}\theta_{c-} \rangle (\cos\sqrt{4\pi}\theta_{s-} + \cos\sqrt{4\pi}\phi_{s-}), \quad (3.4)$$

where g^* means the renormalized value of g . At this fixed point, $K_{s-} \rightarrow 1$ and both perturbations are operators of scaling dimension 1. This system is invariant under the duality transformation $\phi_{s-} \leftrightarrow \theta_{s-}$. This model has been studied extensively in the literature.^{29,48} It is equivalent to a theory of two Ising models. If the coupling constant in front of both operators is the same, as it is the case in Eq. (3.4), one of the Ising models is at its critical point. Equivalently, it can be regarded as a theory of two Majorana fermions, one of which is massive. Hence, this fixed point is in the universality class of the two-dimensional classical Ising model. The Ising order and disorder operators are given by $\sin\sqrt{\pi}\phi_{s-}$ and $\sin\sqrt{\pi}\theta_{s-}$, respectively. At this fixed point, both operators have scaling dimension $1/8$, as they should have at an Ising transition. A small perturbation making $g_3 \gtrless g_4$ or $g_3 \lesseqgtr g_4$ causes a flow towards the CDW+SP or DSC fixed points, respectively. Thus, $g_3=g_4>0$ is the phase boundary between the phase CDW+SP and a d -wave superconductor at $g_{s-}(0)=0$ and $g_{s+}(0)>0$.

However, if the RG flows begin with $g_{s+}(0)<0$ along this direction, then the field ϕ_{s-} is no longer critical. According to Eq. (3.2), in this regime, g_{s+} is marginally relevant and $g_{s+} \rightarrow -\infty$, with $g_3=g_4>0$ and $g_1=g_2<0$. At this fixed point, the fields θ_{c-} and ϕ_{s+} acquire nonvanishing expectation values, and the residual interactions at this fixed point reduce to

$$\begin{aligned} \mathcal{H}_{res}^2 = & \frac{\cos\sqrt{4\pi}\phi_{s-}}{2(\pi a)^2} (g_4^* \langle \cos\sqrt{4\pi}\theta_{c-} \rangle + g_1^* \langle \cos\sqrt{4\pi}\phi_{s+} \rangle) \\ & + \frac{\cos\sqrt{4\pi}\theta_{s-}}{2(\pi a)^2} (g_3^* \langle \cos\sqrt{4\pi}\theta_{c-} \rangle \\ & - g_2^* \langle \cos\sqrt{4\pi}\phi_{s+} \rangle). \end{aligned} \quad (3.5)$$

At this stage of RG, the renormalized couplings satisfy $g_4^* = g_3^*$ and $g_1^* = g_2^*$. Once again we can take

$\langle \cos(\sqrt{4\pi}\theta_{c-}) \rangle = 1$ (the renormalization of its amplitude can be absorbed in a redefined coupling constant). This effective theory has the same form as Eq. (3.4). Hence, this is also a theory of two Ising models. However, unlike Eq. (3.4) the amplitudes of the two dimension one operators are not equal. Hence, generically, both Ising models are off-critical (or equivalently both species of Majorana fermions are massive). This corresponds to a finite correlation length and a finite energy gap at the phase boundary. Hence, in general, this is a first-order transition. If $\langle\phi_{s+}\rangle=0$, then the term of θ_{s-} wins over that of ϕ_{s-} and $g_{s-} \rightarrow +\infty$ in the next step RG transformation. Conversely, if $\langle\phi_{s+}\rangle=\sqrt{\pi}/2$, then the term of ϕ_{s-} wins over that of θ_{s-} and $g_{s-} \rightarrow -\infty$ in the next step RG transformation. Finally, RG flows evolve to the CDW+SP fixed point in the former case while in the latter it does towards the DSC fixed point. Thus, for $g_3=g_4>0$ and $g_{s+}(0)<0$, the phase transition at the boundary of CDW+SP \leftrightarrow DSC becomes first order as the correlation length is now finite. However, a second-order transition is also possible here too. If the spin boson ϕ_{s+} is quantum disordered, then $\langle \cos(\sqrt{4\pi}\phi_{s+}) \rangle = 0$ and once again we get an Ising critical point of the same kind discussed above. Hence, the general conclusion is that this phase boundary may be at a second-order transition (with Ising criticality) or at a first-order transition, with an Ising-like tricritical point in between. Similarly, $g_3=g_4<0$ at $g_{s-}=0$ is the boundary of DDW+DC \leftrightarrow SSC, which is critical and leads to the fixed point at $(0, 0, -\infty, -\infty)$ or to a first order when $g_{s+}>0$ or $g_{s+}<0$, respectively.

Another pair of fixed points $(-\infty, 0, \mp\infty, \pm\infty)$ controls the phase boundaries of the DDW+DC \leftrightarrow DSC transition at $g_3=-g_4<0$, where $\langle\phi_{s+}\rangle=0$, and the phase boundaries of the CDW+SP \leftrightarrow SSC transition at $g_3=-g_4>0$, where $\langle\phi_{s+}\rangle=\sqrt{\pi}/2$; $g_{s+} \rightarrow -\infty$ no matter what its initial value is. The residual interaction for the $s-$ sector is still described by Eq. (3.5) but now with $g_3^* = -g_4^*$. Thus, the amplitudes of $\cos\sqrt{4\pi}\phi_{s-}$ and $\cos\sqrt{4\pi}\theta_{s-}$ are kept equal and this phase boundary is also in the universality class of the Ising critical point. The Ising order and disorder operators can be determined accordingly. The critical phase boundaries are summarized in Table II.

The initial value $g_{s-}(0)$ has important effects on phase boundaries. In Fig. 2, we present the result of a numerical integration of Eq. (3.2) for $g_{s+}(0)>0$; $g_{s-}>0$ favors the growth of $|g_3|$ but disfavors that of $|g_4|$, and conversely $g_{s-}<0$ favors the growth of $|g_4|$ but disfavors that of $|g_3|$. Let us begin with the case $g_{s-}(0)>0$. For $|g_3(0)| \lesseqgtr |g_4(0)|$, at first g_{s-} decreases, then it reaches a positive minimum and finally it increases. Thus, $|g_3|$ increases faster than $|g_4|$ and eventually it wins over it. However, if $|g_3(0)| \ll |g_4(0)|$, g_{s-} decreases monotonically to negative values and $|g_4|$ still wins over $|g_3|$. As a result, both regions of the phase diagram with DDW+DC order and CDW+SP order expand beyond the line $g_3 = \pm g_4$, and the corresponding areas of d -wave and s -wave superconductivities shrink. Due to the symmetry of Eq. (3.2), the situation is reversed for $g_{s-}(0)<0$. For an initial point located on one of these phase boundaries, its RG trajectory flows to the correspond-

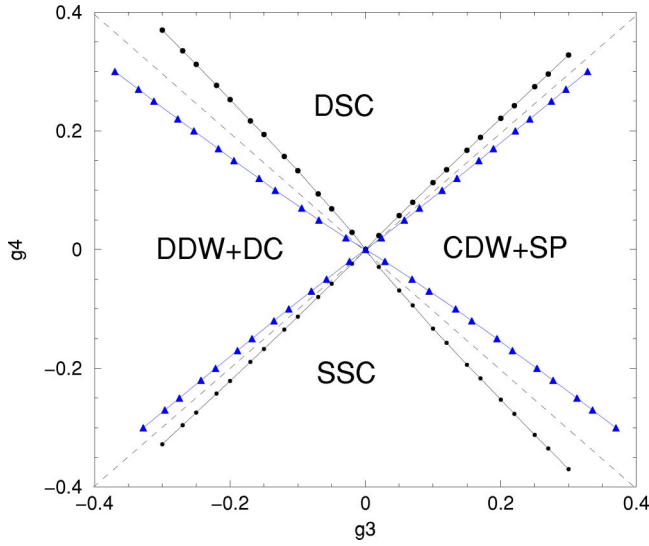


FIG. 2. Phase boundaries with positive initial value of g_{s+} [$g_{s+}(0)=0.2$] and different initial values of $g_{s-}(0)$ with dashed line [$g_{s-}(0)=0$], solid points [$g_{s-}(0)=0.1$], and triangles [$g_{s-}(0)=-0.1$]. Phase boundaries of $CDW+SP \leftrightarrow DSC$, $DDW+DC \leftrightarrow SSC$ become of first order for $g_{s+}(0) < 0$.

ing unstable fixed point, as shown in Fig. 3. For $g_{s+}(0) < 0$, the effect of $g_{s-}(0)$ is similar, but the phase boundaries $CDW+SP \leftrightarrow DSC$ and $DDW+DC \leftrightarrow SSC$ are now first-order transitions and there are no accessible critical points.

We conclude this section with some comments on the DDW phase which has attracted considerable interest recently. Until now, there is no solid numerical evidence away

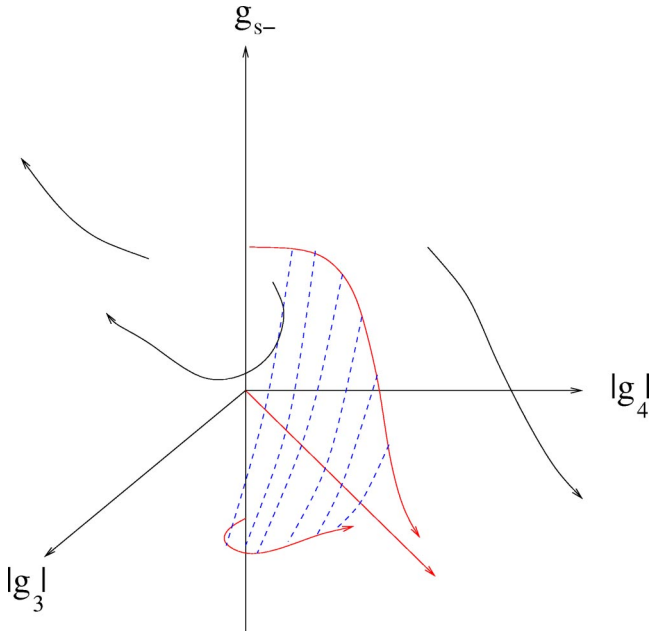


FIG. 3. RG flows in the three-dimensional parameter space with $g_{s+}(0) > 0$. The dashed lines mark the critical surface. $|g_3|$ wins over $|g_4|$ on the left of the surface and $|g_4|$ wins over $|g_3|$ on the right. On the critical surface, the RG trajectories flow to the line $|g_3| = |g_4|$.

from half filling.^{40,42} For the two-leg ladder, we find (see Appendix A) that the DDW phase may exist but it is necessarily incommensurate. We also find V_{\perp} , large and positive, reduces g_4 and enhances g_{s-} , which is favorable for the DDW phase to exist. However, a negative g_3 with magnitude comparable to $|g_4|$ is also needed. Thus, we suggest to look for it in the regimes $V_{\perp} \gg V_d \gg V_{\parallel} > 0$, which has only repulsive interactions, or in $V_{\perp} > 0 > V_{\parallel}$, which has some attractive interactions (and thus is less physically relevant). These arguments agree with the results of a recent two-dimensional mean-field calculation⁴⁴ that the Hubbard U alone cannot stabilize the DDW phase and that negative nearest-neighbor interactions are needed. However, $V_{\perp}, V_{\parallel} < 0$ together favor d -wave superconductivity over the DDW state.

IV. THE PHASE DIAGRAM AT HALF FILLING

Let us now discuss the phase diagram at half filling. The main change is the presence of Umklapp terms. Compared to the incommensurate case discussed in Sec. III, the main difference is that at half filling the \mathbb{Z}_2 symmetries behind two-fold degeneracies found in away from half filling now can be broken spontaneously, with possible phase transitions between the CDW and the spin-Peierls phases, and between the DDW and the DC phases. Since much of the analysis is rather similar, here we will only sketch the main differences.

The set of RG equations is now more complicated:

$$\frac{dK_{c+}}{dl} = -\frac{K_{c+}^2}{8\pi^2}(g_{uc}^2 + g_{u3}^2 + g_{u4}^2 + g_{u5}^2),$$

$$\frac{dK_{c-}}{dl} = \frac{1}{8\pi^2}(g_3^2 + g_4^2 + g_5^2),$$

$$\frac{dK_{s+}}{dl} = -\frac{K_{s+}^2}{8\pi^2}(g_1^2 + g_2^2 + g_5^2 + g_{u5}^2),$$

$$\frac{dK_{s-}}{dl} = -\frac{K_{s-}^2}{8\pi^2}(g_1^2 + g_4^2 + g_{u4}^2) + \frac{1}{8\pi^2}(g_2^2 + g_3^2 + g_{u3}^2),$$

$$\frac{dg_1}{dl} = (2 - K_{s+} - K_{s-})g_1 - \frac{g_4g_5}{2\pi} - \frac{g_{u4}g_{u5}}{2\pi},$$

$$\frac{dg_2}{dl} = \left(2 - K_{s+} - \frac{1}{K_{s-}}\right)g_2 + \frac{g_3g_5}{2\pi} + \frac{g_{u3}g_{u5}}{2\pi},$$

$$\frac{dg_3}{dl} = \left(2 - \frac{1}{K_{c-}} - \frac{1}{K_{s-}}\right)g_3 + \frac{g_2g_5}{2\pi} + \frac{g_{u3}g_{uc}}{2\pi},$$

$$\frac{dg_4}{dl} = \left(2 - \frac{1}{K_{c-}} - K_{s-}\right)g_4 - \frac{g_1g_5}{2\pi} + \frac{g_{u4}g_{uc}}{2\pi},$$

$$\frac{dg_5}{dl} = \left(2 - \frac{1}{K_{c-}} - K_{s+}\right)g_5 - \frac{g_1g_4}{2\pi} + \frac{g_2g_3}{2\pi} + \frac{g_{u5}g_{uc}}{2\pi},$$

$$\begin{aligned}
 \frac{dg_{uc}}{dl} &= \left(2 - K_{c+} - \frac{1}{K_{c-}}\right) g_{uc} + \frac{g_3 g_{u3}}{2\pi} + \frac{g_4 g_{u4}}{2\pi} + \frac{g_5 g_{u5}}{2\pi}, \\
 \frac{dg_{u3}}{dl} &= \left(2 - K_{c+} - \frac{1}{K_{s-}}\right) g_{u3} + \frac{g_2 g_{u5}}{2\pi} + \frac{g_3 g_{uc}}{2\pi}, \\
 \frac{dg_{u4}}{dl} &= (2 - K_{c+} - K_{s-}) g_{u4} - \frac{g_1 g_{u5}}{2\pi} + \frac{g_4 g_{uc}}{2\pi}, \\
 \frac{dg_{u5}}{dl} &= (2 - K_{c+} - K_{s+}) g_{u5} - \frac{g_1 g_{u4}}{2\pi} + \frac{g_2 g_{u3}}{2\pi} + \frac{g_5 g_{uc}}{2\pi}.
 \end{aligned} \tag{4.1}$$

We will not be interested here in solving these RG equations in their full glory, but only in the regime where $K_{c+} \ll 1$ and $K_{c-} \sim 1$. For this range of parameters, there are a number of useful hierarchies of scales which considerably simplify the analysis.

Contrary to what happens away from half filling, the field ϕ_{c+} no longer decouples due to the effects of the Umklapp terms of Eq. (2.5). Clearly, ϕ_{c+} plays a role quite similar to that of θ_{c-} . Indeed, in this regime, g_{uc} is the most relevant coupling and it is associated with an operator with scaling dimension $K_{c+} + 1/K_{c-}$. This operator takes the RG flow close to a fixed point at which the field ϕ_{c+} acquires a gap approximately of the form $m_{c+} \approx a^{-1} |g_{uc}(0)|^{1/(1-K_{c+}(0))}$. In this regime, the field θ_{c-} behaves roughly in the same way as in Eq. (3.2). Here too, the coupling constant g_{c-} flows to strong coupling, $1/K_{c-} \rightarrow 0$, and a gap m_{c-} develops in this sector as it does away from half filling. We will set $\langle \phi_{c+} \rangle = \sqrt{\pi}/2$, correspondingly $\langle \theta_{c-} \rangle = 0$ or $\sqrt{\pi}$ when $g_{uc}(0) > 0$ or < 0 , respectively, so that $\langle \cos \sqrt{4\pi} \phi_{c+} \rangle \approx -(am_{c+})^{K_{c+}(0)}$ and $\langle \cos \sqrt{4\pi} \theta_{c-} \rangle \approx \text{sgn}(g_{uc}) (am_{c-})^{1/K_{c-}(0)}$.

Once the fields ϕ_{c+} and θ_{c-} become pinned close to their classical values, the effective residual interactions among the remaining fluctuating degrees of freedom have an effective Hamiltonian of the form

$$\begin{aligned}
 \mathcal{H}_{eff} &= \frac{\cos \sqrt{4\pi} \phi_{s+}}{2(\pi a)^2} (g_1 \cos \sqrt{4\pi} \phi_{s-} - g_2 \cos \sqrt{4\pi} \theta_{s-}) \\
 &+ \frac{1}{2(\pi a)^2} (g_3^* \cos \sqrt{4\pi} \theta_{s-} + g_4^* \cos \sqrt{4\pi} \phi_{s-} \\
 &+ g_5^* \cos \sqrt{4\pi} \phi_{s+}),
 \end{aligned} \tag{4.2}$$

where $g_{3,4}^*(0) = g_{3,4}(0) \langle \cos \sqrt{4\pi} \theta_{c-} \rangle - g_{u3,u4}(0) \times \langle \cos \sqrt{4\pi} \phi_{c+} \rangle$ and $g_5^*(0) = g_4^*(0) - g_3^*(0)$. If $g_{uc}(0)$ is not small compared to the initial (or bare) values of the other coupling constants, this first step, of the renormalization group flow is rather quick. In this step the marginal coupling constants cannot change very much and thus $|\langle \cos \sqrt{4\pi} \phi_{c+} \rangle| \gg |\langle \cos \sqrt{4\pi} \theta_{c-} \rangle|$ is a good approximation. Hence, the renormalized residual couplings are approximately $(g_3^*, g_4^*, g_5^*) \sim (g_{u3}(0), g_{u4}(0), g_{u5}(0))$.

The new RG equations, which control the subsequent RG flow, are the same as in Eq. (3.2) after setting $1/K_{c-} \rightarrow 0$.

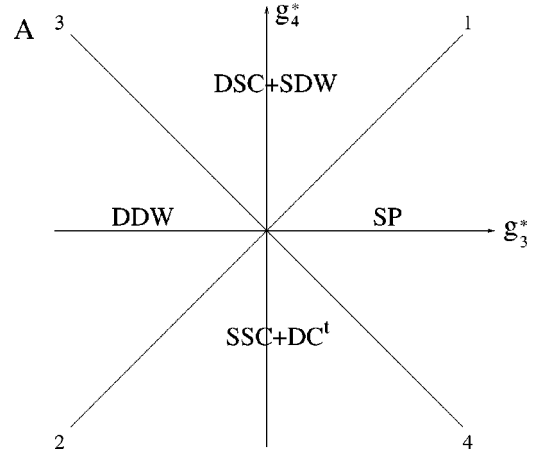


FIG. 4. Stable phases and phase boundaries at half filling with $g_{s-}(0) = 0, g_{s+}(0) > 0$, and $g_{uc}(0) > 0$. Phase boundaries 1,2,5,6 represent first-order transitions when $g_{s+}(0) < 0$. The critical fixed points for the transitions from phases in this figure to their counterparts in Fig. 5 are analogous to those of Fig. 2.

Here too, the SU(2) condition $g_5^* = g_4^* - g_3^*$ is obeyed, albeit among renormalized couplings. The resulting stable phases and the phase boundaries between them are given in the phase diagrams of Figs. 4 and 5. The corresponding stable fixed points and values of pinned fields are summarized in Table III. The critical (or unstable) fixed points are given in Table IV. Umklapp terms break the symmetry group to C_{4v} and thus remove the degeneracy between CDW and SP phases, and between the DDW and DC phases. Hence, all four states become distinct phases with true long-range order, which break the residual Z_2 symmetry spontaneously. At the quantum phase transitions between CDW and SP, and between DDW and DC, the symmetry is U(1).

Perturbative RG studies of Refs. 35 and 36 have described the CDW and DDW fixed points with the property that the coupling constants (written in our notation) satisfy

$$-g_2 = \pm g_3 = \pm g_5 = -g_{u3} = g_{u5} = \mp g_{uc} \rightarrow +\infty,$$

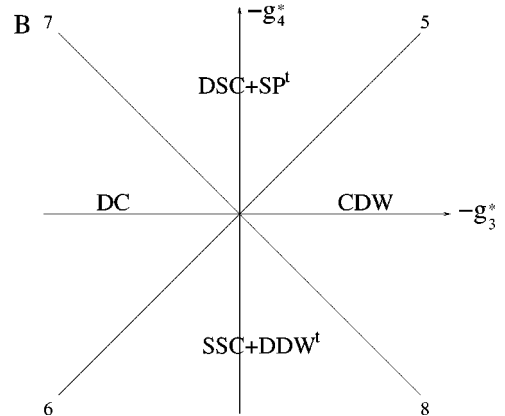


FIG. 5. Phase diagram and boundaries at half filling with $g_{s-}(0) = 0, g_{s+}(0) > 0$, and $g_{uc}(0) < 0$. Note that here we use $-g_3^*$ and $-g_4^*$ as the x, y axes.

TABLE IV. Fixed points at half filling: Unstable fixed points which have the common fixed value $g_{s-}=0$. Here too, $\langle\phi_{c+}\rangle = \sqrt{\pi}/2$, and the SU(2) condition requires $g_5^* = g_4^* - g_3^*$. The column on the right indicates which transition is controlled by each unstable fixed point.

| | g_{uc} | g_{s+} | g_3^*, g_4^*, g_5^* | θ_{c-} | ϕ_{s+} | Transition |
|---|-----------|-----------|-----------------------------|------------------------|------------------------|--------------------------------|
| 1 | $+\infty$ | 0 | $+\infty, +\infty, 0$ | 0 | / | DSC+SDW \leftrightarrow SP |
| 2 | $+\infty$ | 0 | $-\infty, -\infty, 0$ | 0 | / | SSC+DC' \leftrightarrow DDW |
| 3 | $+\infty$ | $-\infty$ | $-\infty, +\infty, +\infty$ | 0 | $\frac{\sqrt{\pi}}{2}$ | DSC+SDW \leftrightarrow DDW |
| 4 | $+\infty$ | $-\infty$ | $+\infty, -\infty, -\infty$ | 0 | 0 | SSC+DC' \leftrightarrow SP |
| 5 | $-\infty$ | 0 | $-\infty, -\infty, 0$ | $\frac{\sqrt{\pi}}{2}$ | / | DSC+SP' \leftrightarrow CDW |
| 6 | $-\infty$ | 0 | $+\infty, +\infty, 0$ | $\frac{\sqrt{\pi}}{2}$ | / | SSC+DDW' \leftrightarrow DC |
| 7 | $-\infty$ | $-\infty$ | $+\infty, -\infty, -\infty$ | $\frac{\sqrt{\pi}}{2}$ | 0 | DSC+SP' \leftrightarrow DC |
| 8 | $-\infty$ | $-\infty$ | $-\infty, +\infty, +\infty$ | $\frac{\sqrt{\pi}}{2}$ | $\frac{\sqrt{\pi}}{2}$ | SSC+DDW' \leftrightarrow CDW |

$$g_1 = g_4 = g_{u4} = 0, \quad (4.3)$$

where the upper (lower) sign holds for the CDW (DDW) phase. It turns out that a model with this particular choice of coupling constants was proposed by Scalapino, Zhang and Hanke (SZH) (Ref. 34) as a ladder model of the SO(5) theory. However, Lin, Balents, and Fisher found that, at least to one-loop order in a perturbative RG (Ref. 35), the symmetry is enlarged actually to SO(8). Moreover, these authors found, also within a perturbative RG, that the SO(8) manifold is at least locally stable, i.e., small deviations from this trajectory converge to this trajectory under the RG flow. Interestingly, the SO(8) manifold is an integrable fermionic system for which a number of exact properties have been calculated using the Bethe Ansatz.⁴⁹ SO(8) is clearly a dynamical symmetry which is possible because all the operators that are involved (back in the fermionic representation) are of dimension two, they are superficially marginal but become marginally relevant due to fluctuations leading to the development of a gap.

However, for more generic values of the coupling constants this dynamical symmetry does not necessarily arise. It is not known that how large the basin of attraction of the SO(8) manifold actually is. In fact, using bosonization methods, we find that far away from the SO(8) manifold, the scaling dimensions of these operators begin to differ significantly from each other and thus evolve differently under the RG [see Eq. (4.3)]. In particular, by checking their scaling dimensions, we find that the renormalized couplings can renormalize differently from each other as

$$|g_2| \ll |g_3| = |g_5| \ll |g_{u3}| = |g_{u4}| \ll |g_c| \rightarrow \infty$$

$$g_1, g_4, g_{u4} \rightarrow 0 \quad (4.4)$$

in all the four phases of CDW, DDW, SP, and DC (Recall that the signs of the coupling constants change in some of the phases.). Nevertheless, what is clear is that the spectrum found in these more anisotropic (and more generic) regimes is smoothly connected to the multiplets found in the SO(8) limit. In other words, there is no phase transition separating these regimes, but the spectrum is organized differently.

Let us now discuss the phase transitions between the CDW and the SP phases, and the between the DDW and DC and phases, and to the associated critical fixed points. As we noted before, these phase transitions are driven by the Umklapp terms, the most relevant of which is controlled by the coupling constant g_{uc} . Hence, *at the critical point* separating the SP and CDW phases, and the DDW and DC phases, the Umklapp terms are tuned to zero. The critical fixed points coincide with the stable fixed points of the incommensurate CDW+SP phase and DDW+DC phase respectively. In both cases, the transition is controlled by the sign of g_{uc} . We also note that the renormalized coupling constant g_3^* has different signs on both sides of this phase transition. This is because, close to the transition $g_3^* \approx g_3 \langle \cos \sqrt{4\pi} \theta_{c-} \rangle$, and $\langle \theta_{c-} \rangle = 0$ in the SP phase while $\langle \theta_{c-} \rangle = \sqrt{\pi}/2$ in the CDW phase. The same is true for the phase transition between the DDW and the DC phases.

It can be shown that, if only charge interactions are considered,⁵⁰ then $g_{uc} = g_{u3}$ at the bare level. In this regime, the CDW and SP phases are more easily accessible than the DDW and DC phases. There is a strong numerical evidence for a commensurate DDW phase at half filling in a t - J -Hubbard ladder⁴¹ who included Heisenberg-like exchange interactions at the microscopic level. It is easy to see that although the inclusion of microscopic exchange interactions does not lead to a different low-energy theory, it changes the strengths of the different effective couplings. In particular, it makes the DDW phase more accessible. For simplicity, we discuss the conditions of the commensurate DDW phase on the SZH ladder which only includes nonzero interactions U, V_{\perp}, J_{\perp} . The coupling constants are given in the weak interaction limit in Appendix A. Let us suppose that V_{\perp} and $J_{\perp} > 0$. First of all, we need positive g_{c+} to set up the overall repulsive interaction, i.e., $U + 2V_{\perp} > 0$. A large J_{\perp} helps to make $g_{uc} > 0$ and $g_{u3} < 0$ simultaneously i.e., $\frac{1}{4}J_{\perp} > U - V_{\perp} > -\frac{3}{4}J_{\perp}$. But J_{\perp} cannot be too large, otherwise negative g_{s-} suppresses the DDW phase. For $|g_{u3}| > |g_{u4}|$, which can be achieved with $U < 0$, this phase is stabilized. But $|U|$ cannot be too large, otherwise g_{c+} would become negative. The region where the commensurate DDW was found in Ref. 41 agrees with this analysis. Again, we need to keep in mind that this naive analysis only makes sense in the weak-coupling limit, which also neglects effects from many irrelevant operators. Thus, we do not expect this analysis to give a precise location of the phase boundary.

Now we discuss the remaining phases and phase transitions. Upon a careful study of which fields become pinned and what are their allowed expectation values, we conclude that the remaining four phases are actually quantum disordered Haldane-like states. For example, there is a phase in which d -wave superconductivity and the SDW order param-

eters (DSC+SDW) are quantum disordered. The order parameter for DSC is very sensitive to fluctuations in the $c+$ sector since $O_{DSC} \propto e^{i\theta_{c+}}$. Similarly, the x , y , and z components of the SDW order parameter are controlled by fluctuations in the $s\pm$ sector since $\vec{O}_{SDW} \propto (\sin(\sqrt{\pi}\theta_{s-}), \sin(\sqrt{\pi}\theta_{s+}), \cos(\sqrt{\pi}\theta_{s+}))$. At this fixed point, the fields θ_{c+} and $\theta_{s\pm}$ are not pinned and fluctuate wildly. Nevertheless, the remaining fields in the expressions for these order parameters do provide for a finite amplitude even though the fluctuations of both phase and orientation are so strong that the system is quantum disordered. The analysis of other three phases, s -wave superconductivity and triplet DC (SSC+DC t), d -wave superconductor and triplet spin-Peierls (DSC+SP t), and s -wave superconductor and triplet d -density wave (SSC+DDW t), is similar. Because of large charge gaps, the low-energy physics of their spin sector may be described by the corresponding O(3) nonlinear σ model without a Berry phase term, which is quantum disordered.

The phase transition between the DSC+SDW phase and the DSC+SP t phase (see Figs. 4 and 5) is the commensurate limit of the d -wave superconductor found away from half filling. A similar relation holds for the phase transition between the SSC+DC t phase, the SSC+DDW t phase, and the s -wave superconductor.

Finally, let us discuss the unstable fixed points with $|g_3^*| = |g_4^*| \rightarrow \infty, g_{s-} = 0$, summarized in Table IV. The RG flows starting from the phase boundaries with $g_{s+}(0) > 0$ evolve towards these fixed points. At these phase boundaries, the order parameters for CDW, SP, DC, and DDW have power-law correlations and have scaling dimension 3/8 at the fixed points denoted by 1,2,5, and 6, and scaling dimension 1/8 at the fixed points denoted by 3, 4, 7 and 8 (see Figs. 4 and 5). On these phase boundaries, the d -wave and s -wave superconducting order parameters are quantum disordered. Similarly, the SDW, SP t , DC t , and DDW t order parameters have power-law correlations and their scaling dimension is 3/8 at the points 1,2,5,6, but are quantum disordered at points 3,4,7,8. For $g_{s-}(0) = 0$, at these phase boundaries, the renormalized couplings satisfy $|g_3^*| = |g_4^*|$ as before. Nonzero $g_{s-}(0)$ also has similar effects on these phase boundaries: $g_{s-}(0) > (<) 0$ favors phases CDW, SP, DC, and DDW (DSC+SDW, SSC+DC t , DSC+SP t , and SSC+DDW t), respectively. When $g_{s+}(0) < 0$, the situation is similar except that transitions 1,2,5,6 become the first order and there are no corresponding unstable fixed points.

V. CONCLUSIONS

In summary, in this paper, we studied the problem of competing orders in two-leg ladders, which were mapped to two-coupled Luttinger liquids with p - h symmetry at both low doping and at half filling. We used (Abelian) bosonization and RG methods to study the phase diagrams of these ladders both at half filling and at low doping. Stable and unstable fixed points of the RG flows with the corresponding phases and phase boundaries were investigated in detail. First-order transitions when $g_{s+}(0) < 0$ are found and the

effects of $g_{s-}(0)$ on phase boundaries are discussed. The $C_{\infty v}$ symmetry makes CDW and spin-Peierls, DC and DDW degenerate. In the absence of Umklapp terms, there is an incommensurate quasi-long-range order. These degeneracies are removed at half filling where true long-range order appears. Power-law fluctuating d -wave and s -wave superconducting phases at low doping levels become quantum disordered at half filling, with finite amplitudes among DSC, SSC and SDW, DC t , SP t , DDW t , respectively. Suggestions on how to best find these phases in numerical simulations were given.

After this paper was submitted for publication, we became aware of the work by Tsuchiizu and Furusaki on a very similar model (at half filling).⁴⁶ In this work, these authors also obtained the same eight insulating phases we found here at half filling. Also after this work was submitted, we learned of the numerical work by Schollwock *et al.*⁵¹ on a DMRG study of a similar ladder model away from the half filling. At low doping, these authors found that their results are consistent with an inhomogeneous picture of the doped state in which the system is locally commensurate. It is our understanding that at long length scales, the system is actually incommensurate with discommensurations (or kinks) separating the locally commensurate regions. On length scales, long compared to the distance between kinks, this state behaves like an effective ‘‘elastic solid’’ which in one dimension has the same quantum critical behavior as a Luttinger liquid. Thus, this state is qualitatively equivalent to our weak-coupling picture, albeit with substantially renormalized parameters.

ACKNOWLEDGMENTS

We thank S. Chakravarty and P. Phillips for helpful discussions. This work was supported by NSF Grant No. DMR98-17941 and Grant No. DMR01-32990 at UIUC. W.V.L. was also supported in part by funds provided by the U.S. Department of Energy (DOE) under Grant No. DF-FC02-94ER40818 at MIT.

APPENDIX A: FERMIONIC HAMILTONIAN

We considered an extended Hubbard model on a ladder with a Hamiltonian of the following form:

$$\begin{aligned}
 H = & -t \sum_{\langle i,j\sigma \rangle} \{c_{i,j\sigma}^\dagger c_{i+1,j\sigma} + \text{H.c.}\} - t_\perp \sum_{\langle i\sigma \rangle} \{c_{i,0\sigma}^\dagger c_{i,1\sigma} + \text{H.c.}\} \\
 & + U \sum_{i,j} n_{i,j\uparrow} n_{i,j\downarrow} + V_\parallel \sum_{i,j} n_{i,j} n_{i+1,j} + V_\perp \sum_i n_{1,i} n_{2,i} \\
 & + V_d \sum_i (n_{i,1} n_{i+1,2} + n_{i,2} n_{i+1,1}) + J_\perp \sum_i \vec{S}_{i,1} \cdot \vec{S}_{i,2} \\
 & + J_\parallel \sum_{ij} \vec{S}_{i,j} \cdot \vec{S}_{i+1,j}. \tag{A1}
 \end{aligned}$$

Here i labels the sites along legs and j labels the legs (or rungs); the coupling constants U , V_\parallel , V_\perp , and V_d represent

the on-site Hubbard interaction and various nearest and next-nearest neighbor Coulomb interactions, and J_{\perp} and J_{\parallel} are the Heisenberg interaction along the rungs and chains, respectively.

After diagonalizing the kinetic part, we can rewrite the

above Hamiltonian with the right and left movers of the bonding and antibonding bands represented by the operators $\psi_{R1}, \psi_{L1}, \psi_{R2}, \psi_{L2}$ as below, where $\psi_{1,2}(x) = (c_{i1} \pm c_{i2})/\sqrt{2a}$. In the low-energy limit, the free part of the continuum Hamiltonian density can be written as

$$\begin{aligned} \mathcal{H}_0 = & v_{f1} \left\{ \frac{\pi}{2} (J_{L1} J_{L1} + J_{R1} J_{R1}) + \frac{2}{3} \pi (\vec{J}_{L1} \cdot \vec{J}_{L1} + \vec{J}_{R1} \cdot \vec{J}_{R1}) \right\} \\ & + v_{f2} \left\{ \frac{\pi}{2} (J_{L2} J_{L2} + J_{R2} J_{R2}) + \frac{2}{3} \pi (\vec{J}_{L2} \cdot \vec{J}_{L2} + \vec{J}_{R2} \cdot \vec{J}_{R2}) \right\}, \end{aligned} \quad (\text{A2})$$

where $J_{i,R,L} = \psi_{i,R,L\sigma}^{\dagger} \psi_{i,R,L\sigma}$ and $\vec{J}_{i,R,L} = \psi_{i,R,L\sigma}^{\dagger} \psi_{i,R,L\sigma}$ are the right and left moving components of the charge and spin current densities for the bonding ($i=1$) and antibonding ($i=2$) fermions, respectively.

The interaction part of the Hamiltonian splits into several terms. First, we have a set of terms involving only the charge currents:

$$\begin{aligned} \mathcal{H}_{int,c} = & \left\{ \frac{U}{8} + \frac{1}{2} (V_{\parallel} + V_d) + \frac{V_{\perp}}{4} \right\} (J_{1R} J_{1R} + J_{1L} J_{1L} + J_{2R} J_{2R} + J_{2L} J_{2L}) + \left\{ \frac{U}{4} + (V_{\parallel} + V_d) \left(1 - \frac{\cos 2k_{f1}}{2} \right) + \frac{V_{\perp}}{4} - \frac{3}{8} \cos 2k_{f1} J_{\parallel} \right. \\ & - \left. \frac{3}{16} J_{\perp} \right\} J_{1R} J_{1L} + \left\{ \frac{U}{4} + (V_{\parallel} + V_d) \left(1 - \frac{\cos 2k_{f2}}{2} \right) + \frac{V_{\perp}}{4} - \frac{3}{8} \cos 2k_{f2} J_{\parallel} - \frac{3}{16} J_{\perp} \right\} J_{2R} J_{2L} + \left\{ \frac{U}{4} + V_{\parallel} \left(1 - \frac{1}{2} \cos k_{-} \right) \right. \\ & + \left. V_d \left(1 + \frac{1}{2} \cos k_{-} \right) + \frac{3}{4} V_{\perp} - \frac{3}{8} J_{\parallel} \cos k_{-} + \frac{3}{16} J_{\perp} \right\} (J_{1R} J_{2R} + J_{1L} J_{2L}) + \left\{ \frac{U}{4} + V_{\parallel} \left(1 - \frac{1}{2} \cos k_{+} \right) + V_d \left(1 + \frac{1}{2} \cos k_{+} \right) \right. \\ & + \left. \frac{3}{4} V_{\perp} - \frac{3}{8} J_{\parallel} \cos k_{+} + \frac{3}{16} J_{\perp} \right\} (J_{1R} J_{2L} + J_{1L} J_{2R}), \end{aligned} \quad (\text{A3})$$

where $k_{+} = k_{f1} + k_{f2} = \pi(1 - \delta)$, and $k_{-} = k_{f1} - k_{f2} = 2 \sin^{-1}[t_{\perp}/(2 \cos \pi \delta/2)]$.

Next we have the couplings involving the spin currents:

$$\begin{aligned} \mathcal{H}_{int,s} = & \left\{ -\frac{U}{6} + \frac{J_{\parallel}}{2} + \frac{J_{\perp}}{4} \right\} (\vec{J}_{1R} \vec{J}_{1R} + \vec{J}_{1L} \vec{J}_{1L} + \vec{J}_{2R} \vec{J}_{2R} + \vec{J}_{2L} \vec{J}_{2L}) - \left\{ U + 2(V_{\parallel} + V_d) \cos 2k_{f1} + V_{\perp} - \frac{3}{4} J_{\perp} \right\} \vec{J}_{1R} \vec{J}_{1L} \\ & - \left\{ U + 2(V_{\parallel} + V_d) \cos 2k_{f2} + V_{\perp} - \frac{3}{4} J_{\perp} \right\} \vec{J}_{2R} \vec{J}_{2L} - \left\{ U + 2(V_{\parallel} - V_d) \cos k_{-} - V_{\perp} - \left(1 + \frac{1}{2} \cos k_{-} \right) J_{\parallel} - \frac{J_{\perp}}{4} \right\} \\ & \times (\vec{J}_{1R} \vec{J}_{2R} + \vec{J}_{1L} \vec{J}_{2L}) - \left\{ U + 2(V_{\parallel} - V_d) \cos k_{+} - V_{\perp} - \left(1 + \frac{1}{2} \cos k_{+} \right) J_{\parallel} - \frac{J_{\perp}}{4} \right\} (\vec{J}_{1R} \vec{J}_{2L} + \vec{J}_{1L} \vec{J}_{2R}). \end{aligned} \quad (\text{A4})$$

Next we have the low-energy couplings associated with singlet-pair and triplet-pair tunnelings:

$$\mathcal{H}_{int,pt} = \left\{ U + \left(2(V_{\parallel} - V_d) - \frac{3}{2} J_{\parallel} \right) \cos k_{f1} \cos k_{f2} - V_{\perp} + \frac{3}{4} J_{\perp} \right\} (\Delta_1^{\dagger} \Delta_2 + \text{H.c.}) + \left\{ 2(V_{\parallel} - V_d) + \frac{J_{\parallel}}{2} \right\} \text{sink}_{f1} \text{sink}_{f2} (\vec{\Delta}_1^{\dagger} \vec{\Delta}_2 + \text{H.c.}) \quad (\text{A5})$$

where $\Delta = (\psi_{R\uparrow} \psi_{L\downarrow} - \psi_{R\downarrow} \psi_{L\uparrow})/\sqrt{2}$ is the singlet-pair operator on a given chain and $\vec{\Delta}$ is its triplet counterpart. Note that 1 and 2 stand here for the chain label.

Finally, the low-energy Umklapp scattering terms are

$$\begin{aligned} \mathcal{H}_{um} = & e^{2i\delta\pi x} \left(\left\{ \frac{U}{4} + e^{i\delta\pi} \left[V_{\parallel} \left(\frac{1}{2} - \cos k_{-} \right) - V_d \left(\frac{1}{2} + \cos k_{-} \right) + \frac{3}{8} J_{\parallel} \right] + \frac{3}{4} V_{\perp} + \frac{3}{16} J_{\perp} \right\} N_1^{\dagger} N_2^{\dagger} \right. \\ & - \left. \left\{ U + e^{i\delta\pi} \left[-2(V_{\parallel} - V_d) + \left(\frac{1}{2} + \cos k_{-} \right) J_{\parallel} \right] - V_{\perp} - \frac{J_{\perp}}{4} \right\} \vec{N}_1^{\dagger} \vec{N}_2^{\dagger} + \left\{ \frac{U}{2} - \left(V_{\parallel} - V_d - \frac{3}{4} J_{\parallel} \right) e^{i\delta\pi} - \frac{V_{\perp}}{2} + \frac{3}{8} J_{\perp} \right\} \right. \\ & \left. \times (m_{1R}^{\dagger} m_{2L} + m_{2R}^{\dagger} m_{1L}) \right) + \text{H.c.}, \end{aligned} \quad (\text{A6})$$

Here $N^\dagger = \psi_{R\sigma}^\dagger \psi_{L\sigma}$ and $\vec{N}^\dagger = \psi_{R\sigma}^\dagger (\vec{\sigma}/2) \psi_{L\sigma}$ are CDW and SDW (Néel) order parameters, respectively. m is the pairing order with $2k_f$ momentum, for example, $m_R = \psi_{R,\uparrow} \psi_{R,\downarrow}$.

Following the standard Bosonization procedure with the assumption of Eq. (2.1), we arrive at the bosonized Hamiltonian density in the Sec. II. The bare values of the weak-coupling constants are given as

$$\begin{aligned}
g_{c+} &= U + V_{\parallel} [4 + \cos \pi \delta (1 + \cos k_{f-})] + 2V_{\perp} + V_d [4 - \cos \pi \delta (1 - \cos k_{f-})] + \frac{3}{4} J_{\parallel} \cos \pi \delta (1 + \cos k_{-}), \\
g_{c-} &= - \left(V_{\parallel} + \frac{3}{4} J_{\parallel} \right) \cos \pi \delta (1 - \cos k_{f-}) - V_{\perp} + \cos \pi \delta (1 + \cos k_{f-}) V_d - \frac{3}{4} J_{\perp}, \\
g_{s+} &= U - V_{\parallel} \cos \pi \delta (1 + \cos k_{f-}) + V_d \cos \pi \delta (1 - \cos k_{f-}) - \frac{J_{\parallel}}{2} \left(1 - \frac{1}{2} \cos \pi \delta \right) - \frac{J_{\perp}}{2}, \\
g_{s-} &= V_{\parallel} \cos \pi \delta (1 - \cos k_{f-}) + V_{\perp} - V_d \cos \pi \delta (1 + \cos k_{f-}) + \frac{J_{\parallel}}{2} \left(1 - \frac{1}{2} \cos \pi \delta \right) - \frac{1}{4} J_{\perp}, \\
g_3 &= 2 \left(V_{\parallel} - V_d + \frac{J_{\parallel}}{4} \right) [\cos k_{-} + \cos \pi \delta], g_4 = U + 2(V_{\parallel} - V_d) \cos k_{-} - V_{\perp} + J_{\parallel} \left(\cos \pi \delta - \frac{1}{2} \cos k_{-} \right) + \frac{3}{4} J_{\perp}, \\
g_{uc} &= U - 2 \cos \pi \delta \left(V_{\parallel} - V_d - \frac{3}{2} J_{\parallel} \right) - V_{\perp} + \frac{3}{4} J_{\perp}, g_{u3} = U - 2 \cos \pi \delta \left[V_{\parallel} - V_d - J_{\parallel} \left(\frac{1}{4} + \frac{1}{2} \cos k_{-} \right) \right] - V_{\perp} - \frac{J_{\perp}}{4}, \\
g_{u4} &= U - 2 \cos \pi \delta \left[(V_{\parallel} + V_d) \cos k_{-} - J_{\parallel} \left(1 + \frac{1}{2} \cos k_{-} \right) \right] + V_{\perp} + \frac{J_{\perp}}{4}, \\
g_1 &= g_{s+} + g_{s-}, \quad g_2 = g_{s+} - g_{s-}, \\
g_5 &= g_4 - g_3, \quad g_{u5} = g_{u4} - g_{u3},
\end{aligned} \tag{A7}$$

where $\cos k_{-} = 1 - t_{\perp}^2 / (2t^2)$. Up to the first order, these coupling constants are independent of the doping δ .

When away from the half filling, the particle-hole symmetry Eq. (2.1) only holds approximately at small doping δ as $k_{+} - \pi = \delta \pi, \Delta v_f / a = \delta t_{\perp} \pi$. Taking these into account, there are some small residue terms as appearing in Eqs. (2.6), (2.7), and (2.8), they vanish linearly with doping. The corresponding coupling constants are

$$\begin{aligned}
\Delta g_c &= \left\{ \frac{1}{2} (V_{\parallel} + V_d) + \frac{3}{8} J_{\parallel} \right\} \sin \pi \delta \sin k_{f-}, \\
\Delta g_s &= - \frac{1}{2} (V_{\parallel} + V_d) \sin \pi \delta \sin k_{f-}, \\
\Delta g_{uc} &= - 2 \sin \pi \delta \left(V_{\parallel} - V_d - \frac{3}{4} J_{\parallel} \right), \\
\Delta g_{u3} &= - 2 \sin \pi \delta \left[V_{\parallel} - V_d - J_{\parallel} \left(\frac{1}{4} + \frac{\cos k_{-}}{2} \right) \right] \\
\Delta g_{u4} &= - 2 \sin \pi \delta \left[(V_{\parallel} + V_d) \cos k_{-} - J_{\parallel} \left(1 + \frac{1}{2} \cos k_{-} \right) \right], \quad \Delta g_{u5} = \Delta g_{u3} - \Delta g_{u4}.
\end{aligned} \tag{A8}$$

APPENDIX B: BOSONIC REPRESENTATION OF THE ORDER PARAMETERS

The difference of the charge density between two legs reads $\sum_{\sigma} (-)^{j+1} c_{j\sigma}^{\dagger}(i) c_{j\sigma}(i) = \sum_{\sigma} \psi_{1\sigma}^{\dagger}(x) \psi_{2\sigma}(x) + \psi_{2\sigma}^{\dagger}(x) \psi_{1\sigma}(x)$. After expressed by the right and left movers, it contains the staggered part, i.e., O_{CDW} . A similar situation happens to its triplet counterpart $O_{SDW,z,x,y}$. Using the bosonization identities $\psi_{R,L}(x) = 1/\sqrt{2\pi a} \exp\{\pm i\sqrt{\pi}(\phi(x) \pm \theta(x))\}$ and we can obtain their bosonic expressions as below:

$$\begin{aligned}
 \left. \begin{aligned} O_{CDW}(x) \\ \vec{O}_{SDW,z,x,y}(x) \end{aligned} \right\} &= (-)^x e^{-i\delta\pi x} \left\{ \begin{aligned} &\psi_{1L\sigma}^\dagger(x) \psi_{2R\sigma}(x) + \psi_{2L\sigma}^\dagger(x) \psi_{1R\sigma}(x) + \text{H.c.} \\ &\psi_{1L\alpha}^\dagger(x) (\vec{\sigma}/2)_{\alpha\beta} \psi_{2R\beta}(x) + \psi_{2L\alpha}^\dagger(x) (\vec{\sigma}/2)_{\alpha\beta} \psi_{1R\beta}(x) + \text{H.c.} \end{aligned} \right. \\
 &\propto \frac{2\Gamma}{\pi a} \{ \cos(\sqrt{\pi}\phi_{c+} - \delta\pi x) \} \left\{ \begin{aligned} &2 \cos\sqrt{\pi}\theta_{c-} \cos\sqrt{\pi}\phi_{s+} \sin\sqrt{\pi}\theta_{s-} \\ &\sin\sqrt{\pi}\theta_{c-} \begin{cases} \cos\sqrt{\pi}\phi_{s+} \cos\sqrt{\pi}\theta_{s-} \\ \cos\sqrt{\pi}\theta_{s+} \cos\sqrt{\pi}\phi_{s-} \\ -\sin\sqrt{\pi}\theta_{s+} \cos\sqrt{\pi}\phi_{s-} \end{cases} + \sin(\sqrt{\pi}\phi_{c+} - \delta\pi x) \end{aligned} \right. \\
 &\times \left\{ \begin{aligned} &-2 \sin\sqrt{\pi}\theta_{c-} \sin\sqrt{\pi}\phi_{s+} \cos\sqrt{\pi}\theta_{s-} \\ &-\cos\sqrt{\pi}\theta_{c-} \begin{cases} \sin\sqrt{\pi}\phi_{s+} \sin\sqrt{\pi}\theta_{s-} \\ \sin\sqrt{\pi}\theta_{s+} \sin\sqrt{\pi}\phi_{s-} \\ \cos\sqrt{\pi}\theta_{s+} \sin\sqrt{\pi}\phi_{s-} \end{cases} \end{aligned} \right\}, \tag{B1}
 \end{aligned}$$

where Γ equals $i\eta_\uparrow(1)\eta_\uparrow(2)$ for the singlet and z component of the triplet-order parameters, and $i\eta_\uparrow(1)\eta_\downarrow(2)$ for x, y components of the triplet-order parameters, and the same as below.

The difference of the bond strength between two legs is $\sum_{j\sigma} (-)^{j+1} c_{j\sigma}^\dagger(i) c_{j\sigma}(i+1) + \text{H.c.} = \sum_\sigma \psi_{1\sigma}^\dagger(x) \psi_{2\sigma}(x+a) + \psi_{2\sigma}^\dagger(x) \psi_{1\sigma}(x+a) + \text{H.c.}$, similar is its triplet analog. Their staggered parts O_{SP} and \vec{O}_{SP}^t are the following:

$$\begin{aligned}
 \left. \begin{aligned} O_{SP}(x) \\ \vec{O}_{SP,z,x,y}^t(x) \end{aligned} \right\} &= (-)^x 2 \sin\left(k_{f1} + \frac{\pi}{2} \delta\right) i \left\{ e^{-i\pi\delta x - i\delta\pi/2} \left\{ \begin{aligned} &\psi_{1L\sigma}^\dagger(x) \psi_{2R\sigma}(x) + \psi_{2L\sigma}^\dagger(x) \psi_{1R\sigma}(x) - \text{H.c.} \\ &\psi_{1L\alpha}^\dagger(x) (\vec{\sigma}/2)_{\alpha\beta} \psi_{2R\beta}(x) + \psi_{2L\alpha}^\dagger(x) (\vec{\sigma}/2)_{\alpha\beta} \psi_{1R\beta}(x) - \text{H.c.} \end{aligned} \right. \right. \\
 &\propto \frac{2\Gamma}{\pi a} \{ \cos(\sqrt{\pi}\phi_{c+} - \delta\pi x - \delta\pi/2) \} \left\{ \begin{aligned} &2 \sin\sqrt{\pi}\theta_{c-} \sin\sqrt{\pi}\phi_{s+} \cos\sqrt{\pi}\theta_{s-} \\ &\cos\sqrt{\pi}\theta_{c-} \begin{cases} \sin\sqrt{\pi}\phi_{s+} \sin\sqrt{\pi}\theta_{s-} \\ \sin\sqrt{\pi}\theta_{s+} \sin\sqrt{\pi}\phi_{s-} \\ \cos\sqrt{\pi}\theta_{s+} \sin\sqrt{\pi}\phi_{s-} \end{cases} \end{aligned} \right. \\
 &+ \sin(\sqrt{\pi}\phi_{c+} - \delta\pi x - \delta\pi/2) \left\{ \begin{aligned} &2 \cos\sqrt{\pi}\theta_{c-} \cos\sqrt{\pi}\phi_{s+} \sin\sqrt{\pi}\theta_{s-} \\ &\sin\sqrt{\pi}\theta_{c-} \begin{cases} \cos\sqrt{\pi}\phi_{s+} \cos\sqrt{\pi}\theta_{s-} \\ \cos\sqrt{\pi}\theta_{s+} \cos\sqrt{\pi}\phi_{s-} \\ -\sin\sqrt{\pi}\theta_{s+} \cos\sqrt{\pi}\phi_{s-} \end{cases} \end{aligned} \right\}. \tag{B2}
 \end{aligned}$$

It is clear that O_{CDW} and O_{SP} are real and imaginary parts of $\psi_{1L\sigma}^\dagger \psi_{2R\sigma} + \psi_{2L\sigma}^\dagger \psi_{1R\sigma}$, respectively.

Next we present the staggered part of the diagonal current density, $i\sum_j (-)^{j+1} c_j^\dagger(i) c_{j+1}(i+1) - \text{H.c.}$, and its triplet analog as below:

$$\begin{aligned}
 \left. \begin{aligned} O_{DC}(x) \\ \vec{O}_{DC,z,x,y}^t(x) \end{aligned} \right\} &= (-)^x \sin(k_{f1} + \delta\pi/2) \left\{ e^{-i\pi\delta x - i\delta/2\pi} \left\{ \begin{aligned} &\psi_{1L\sigma}^\dagger(x) \psi_{2R\sigma}(x) - \psi_{2L\sigma}^\dagger(x) \psi_{1R\sigma}(x) + \text{H.c.} \\ &\psi_{1L\alpha}^\dagger(x) (\vec{\sigma}/2)_{\alpha\beta} \psi_{2R\beta}(x) - \psi_{2L\alpha}^\dagger(x) (\vec{\sigma}/2)_{\alpha\beta} \psi_{1R\beta}(x) + \text{H.c.} \end{aligned} \right. \right. \\
 &\propto \frac{2\Gamma}{\pi a} \left\{ \cos\left(\sqrt{\pi}\phi_{c+} - \pi\delta x - \frac{\delta\pi}{2}\right) \right\} \left\{ \begin{aligned} &2 \cos\sqrt{\pi}\theta_{c-} \sin\sqrt{\pi}\phi_{s+} \cos\sqrt{\pi}\theta_{s-} \\ &-\sin\sqrt{\pi}\theta_{c-} \begin{cases} \sin\sqrt{\pi}\phi_{s+} \sin\sqrt{\pi}\theta_{s-} \\ \sin\sqrt{\pi}\theta_{s+} \sin\sqrt{\pi}\phi_{s-} \\ \cos\sqrt{\pi}\theta_{s+} \sin\sqrt{\pi}\phi_{s-} \end{cases} \end{aligned} \right. \\
 &+ \sin\left(\sqrt{\pi}\phi_{c+} - \pi\delta x - \frac{\delta\pi}{2}\right) \left\{ \begin{aligned} &-2 \sin\sqrt{\pi}\theta_{c-} \cos\sqrt{\pi}\phi_{s+} \sin\sqrt{\pi}\theta_{s-} \\ &\cos\sqrt{\pi}\theta_{c-} \begin{cases} \cos\sqrt{\pi}\phi_{s+} \cos\sqrt{\pi}\theta_{s-} \\ \cos\sqrt{\pi}\theta_{s+} \cos\sqrt{\pi}\phi_{s-} \\ -\sin\sqrt{\pi}\theta_{s+} \cos\sqrt{\pi}\phi_{s-} \end{cases} \end{aligned} \right\}. \tag{B3}
 \end{aligned}$$

The difference of the current density along the legs is $i\sum_j (-)^{j+1} [c_{j\sigma}^\dagger(i) c_{j\sigma}(i+1) - \text{H.c.}]$. Its staggered part is

$$(-)^x 2 \cos\left(k_{1f} + \frac{\delta\pi}{2}\right) (-i) \sum_{\sigma} \left\{ e^{-i\pi\delta x - i\delta\pi/2} (\psi_{1\sigma L}^{\dagger}(x) \psi_{2\sigma R}(x) - \psi_{2\sigma L}^{\dagger}(x) \psi_{1\sigma R}(x)) - \text{H.c.} \right\}.$$

Similarly, the staggered current along the rung $i[c_{2\sigma}^{\dagger}(i)c_{1\sigma}(i) - \text{H.c.}]$ is

$$(-)^x t_{\perp} \left\{ \frac{i}{2} \sum_{\delta} e^{-i\pi\delta x} (\psi_{1\sigma L}^{\dagger} \psi_{2\sigma R} - \psi_{2\sigma L}^{\dagger} \psi_{1\sigma R}) - \text{H.c.} \right\}.$$

It can be shown that they satisfy the continuous relation,³⁶ so does its triplet counterpart, \vec{O}_{DDW} staggered currents along legs and rungs have the d -wave feature. We use currents along the rung as order parameters. Their bosonized forms are

$$\begin{aligned} \left. \begin{aligned} O_{DDW}(x) \\ \vec{O}_{DDW^{t,z,x,y}}(x) \end{aligned} \right\} &\propto \frac{2\Gamma}{\pi a} \left\{ \cos(\sqrt{\pi}\phi_{c+} - \pi\delta x) \begin{cases} 2\sin\sqrt{\pi}\theta_{c-} \cos\sqrt{\pi}\phi_{s+} \sin\sqrt{\pi}\theta_{s-} \\ -\cos\sqrt{\pi}\theta_{c-} \begin{cases} \cos\sqrt{\pi}\phi_{s+} \cos\sqrt{\pi}\theta_{s-} \\ \cos\sqrt{\pi}\theta_{s+} \cos\sqrt{\pi}\phi_{s-} \\ -\sin\sqrt{\pi}\theta_{s+} \cos\sqrt{\pi}\phi_{s-} \end{cases} + \sin(\sqrt{\pi}\phi_{c+} - \pi\delta x) \end{cases} \right. \\ &\times \left. \begin{cases} 2\cos\sqrt{\pi}\theta_{c-} \sin\sqrt{\pi}\phi_{s+} \cos\sqrt{\pi}\theta_{s-} \\ -\sin\sqrt{\pi}\theta_{c-} \begin{cases} \sin\sqrt{\pi}\phi_{s+} \sin\sqrt{\pi}\theta_{s-} \\ \sin\sqrt{\pi}\theta_{s+} \sin\sqrt{\pi}\phi_{s-} \\ \cos\sqrt{\pi}\theta_{s+} \sin\sqrt{\pi}\phi_{s-} \end{cases} \end{cases} \right\}. \end{aligned} \quad (\text{B4})$$

It can also be seen that the DC and DDW order parameters are the real and imaginary parts of $\psi_{1L\sigma}^{\dagger} \psi_{2R\sigma} - \psi_{2L\sigma}^{\dagger} \psi_{1R\sigma}$, respectively.

Finally, the bosonized forms of the d -wave and s -wave pairing order parameters are

$$\begin{aligned} \Delta_d &= (\psi_{1L\uparrow} \psi_{1R\downarrow} - \psi_{1L\downarrow} \psi_{1R\uparrow}) - (\psi_{2L\uparrow} \psi_{2R\downarrow} - \psi_{2L\downarrow} \psi_{2R\uparrow}) \\ &= \frac{2\eta_{\uparrow}(1)\eta_{\downarrow}(1)}{\pi a} e^{i\sqrt{\pi}\theta_{c+}} (-\cos\sqrt{\pi}\theta_{c-} \sin\sqrt{\pi}\phi_{s+} \sin\sqrt{\pi}\phi_{s-} + i \sin\sqrt{\pi}\theta_{c-} \cos\sqrt{\pi}\phi_{s+} \cos\sqrt{\pi}\phi_{s-}), \\ \Delta_s &= (\psi_{1L\uparrow} \psi_{1R\downarrow} - \psi_{1L\downarrow} \psi_{1R\uparrow}) + (\psi_{2L\uparrow} \psi_{2R\downarrow} - \psi_{2L\downarrow} \psi_{2R\uparrow}) \\ &= \frac{2\eta_{\uparrow}(1)\eta_{\downarrow}(1)}{\pi a} e^{i\sqrt{\pi}\theta_{c+}} (\cos\sqrt{\pi}\theta_{c-} \cos\sqrt{\pi}\phi_{s+} \cos\sqrt{\pi}\phi_{s-} + i \sin\sqrt{\pi}\theta_{c-} \sin\sqrt{\pi}\phi_{s+} \sin\sqrt{\pi}\phi_{s-}). \end{aligned} \quad (\text{B5})$$

-
- ¹S.C. Zhang, Science **275**, 1089 (1997).
²V.J. Emery, S.A. Kivelson, and O. Zachar, Phys. Rev. B **56**, 6120 (1997).
³S.A. Kivelson, E. Fradkin, and V.J. Emery, Nature (London) **393**, 550 (1998).
⁴Mats Granath, Vadim Oganesyan, Steven A. Kivelson, Eduardo Fradkin, and Victor J. Emery, Phys. Rev. Lett. **87**, 167011 (2001).
⁵I.K. Affleck and J.B. Marston, Phys. Rev. B **37**, 3774 (1988).
⁶X.-G. Wen and P.A. Lee, Phys. Rev. Lett. **76**, 503 (1996).
⁷Chetan Nayak, Phys. Rev. B **62**, 4880 (2000).
⁸S. Chakravarty, R.B. Laughlin, Dirk K. Morr, and Chetan Nayak, Phys. Rev. B **63**, 094503 (2001).
⁹C.M. Varma, Phys. Rev. B **55**, 14554 (1997); Phys. Rev. Lett. **83**, 3538 (1999).
¹⁰C.J. Wu and W.V. Liu, Phys. Rev. B **66**, 020511(R) (2002).
¹¹S.A. Kivelson, D. Rokhsar, and J.P. Sethna, Phys. Rev. B **35**, 8865 (1987).
¹²P.W. Anderson, Science **235**, 1196 (1987); G. Baskaran and P.W. Anderson, Phys. Rev. B **37**, 580 (1988).
¹³V. Kalmeyer and R.B. Laughlin, Phys. Rev. Lett. **59**, 2095 (1988); X.G. Wen, F. Wilczek, and A. Zee, Phys. Rev. B **39**, 11 413 (1989).
¹⁴G. Kotliar and J. Liu, Phys. Rev. B **38**, 5142 (1988).
¹⁵T.C. Hsu, J.B. Marston, and I. Affleck, Phys. Rev. B **43**, 2866 (1991).
¹⁶M.U. Ubbens and P.A. Lee, Phys. Rev. B **49**, 6853 (1994).
¹⁷L. Balents, M.P.A. Fisher, and C. Nayak, Int. J. Mod. Phys. B **12**, 1033 (1998).
¹⁸J. Zaanen and O. Gunnarsson, Phys. Rev. B **40**, 7391 (1989).
¹⁹H.J. Schulz, Phys. Rev. Lett. **64**, 1445 (1990).
²⁰E.W. Carlson, S.A. Kivelson, Z. Nussinov, and V.J. Emery, Phys. Rev. B **57**, 14 704 (1998).

- ²¹M. Vojta, Y. Zhang, and S. Sachdev, Phys. Rev. B **62**, 6721 (2000); K. Park and S. Sachdev, *ibid.* **64**, 184510 (2001).
- ²²Chetan Nayak and Eugene Pivovarov, Phys. Rev. B **66**, 064508 (2002).
- ²³C. Mudry and E. Fradkin, Phys. Rev. B **49**, 5200 (1994); see also C. Mudry and E. Fradkin, *ibid.* **50**, 11 409 (1994) for a discussion of spin-charge separation in $d=1$.
- ²⁴T. Senthil and M.P.A. Fisher, Phys. Rev. B **62**, 7850 (2000).
- ²⁵R. Moessner and S.L. Sondhi, Phys. Rev. B **66**, 1881 (2001).
- ²⁶C.M. Varma and A. Zawadowski, Phys. Rev. B **32**, 7399 (1985).
- ²⁷M. Fabrizio, Phys. Rev. B **48**, 15 838 (1993).
- ²⁸D.V. Khveshchenko and T.M. Rice, Phys. Rev. B **50**, 252 (1994).
- ²⁹H.J. Schulz, Phys. Rev. B **53**, R2959 (1996).
- ³⁰E. Orignac and T. Giamarchi, Phys. Rev. B **56**, 7167 (1997).
- ³¹D. Shelton and D. Senechal, Phys. Rev. B **58**, 6818 (1998).
- ³²L. Balents and M.P.A. Fisher, Phys. Rev. B **53**, 12 133 (1996).
- ³³A.O. Gogolin, A.A. Nersesyan, and A.M. Tsvelik, *Bosonization and Strongly Correlated Systems* (Cambridge University Press, Cambridge, 1998).
- ³⁴D.J. Scalapino, S.-C. Zhang, and W. Hanke, Phys. Rev. B **58**, 443 (1998).
- ³⁵H.H. Lin, L. Balents, and M.P.A. Fisher, Phys. Rev. B **58**, 1794 (1998).
- ³⁶J.O. Fjarestad and J.B. Marston, Phys. Rev. B **65**, 125106 (2002).
- ³⁷S. White and D.J. Scalapino, Phys. Rev. B **57**, 3031 (1998).
- ³⁸E. Dagotto, J. Riera, and D.J. Scalapino, Phys. Rev. B **45**, 5744 (1992).
- ³⁹R.M. Noack, N. Bulut, D.J. Scalapino, and M.G. Zacher, Phys. Rev. B **56**, 7162 (1997); T.M. Rice, Stephan Haas, and Manfred Sigrist, *ibid.* **56**, 14 655 (1997).
- ⁴⁰D.J. Scalapino, S.R. White, and I.K. Affleck, Phys. Rev. B **64**, 100506 (2001).
- ⁴¹J.B. Marston, J.O. Fjarestad and Asle Sudbo, Phys. Rev. Lett. **89**, 056404 (2002).
- ⁴²M. Troyer, S. Chakravarty, and Uli Schollwöck, Bull. Am. Phys. Soc. **47**, 347 (2002).
- ⁴³For an overview on the physics of two-leg materials see E. Dagotto and T.M. Rice, Science **271**, 618 (1996).
- ⁴⁴T.D. Stanescu and P.W. Phillips, Phys. Rev. B **64**, 220509 (2001).
- ⁴⁵V.J. Emery, S.A. Kivelson, and O. Zachar, Phys. Rev. B **59**, 15 641 (1999).
- ⁴⁶M. Tsuchiizu, and A. Furusaki, Phys. Rev. B **66**, 245106 (2002).
- ⁴⁷T. Giamarchi, Phys. Rev. B **44**, 2905 (1991).
- ⁴⁸P. Lecheminant, A.O. Gogolin, and A.A. Nersesyan, Nucl. Phys. B **639**, 502 (2002).
- ⁴⁹R. Konik, F. Leasage, A.W.W. Ludwig, and H. Saleur, Phys. Rev. B **61**, 4983 (2000); R. Konik and A.W.W. Ludwig, *ibid.* **64**, 155112 (2001).
- ⁵⁰ $g_{uc} = g_u/3 = 1/N \sum_{\vec{r}} (-)^{r_x+r_y} V(\vec{r})$ for two-leg ladder with an arbitrary charge interaction $V(\vec{r})$.
- ⁵¹U. Schollwöck, S. Chakravarty, J.O. Fjarestad, J.B. Marston, and M. Troyer, Phys. Rev. Lett. **90**, 186401 (2003).